DISCLAIMER

This contractor document was prepared for the U.S. Department of Energy (DOE), but has not undergone programmatic, policy, or publication review, and is provided for information only. The document provides preliminary information that may change based on new information to be used specifically for Total System Performance Assessment analyses. The document is a preliminary lower-level contractor document and is not intended for publication or wide distribution.

Although this document has undergone technical reviews at the contractor organization, it has not undergone a DOE policy review. Therefore, the views and options of authors expressed may not state or reflect those of the DOE. However, in the interest of the rapid transfer of information, we are providing this document for your information per your request.

OFFICE OF CIVILIAN RADIOACTIVE WASTE MANAGEMENT
ANALYSIS/MODEL COVER SHEET
Complete Only Applicable Items

1. QA: QA

2. ☒ Analysis — Check all that apply

Type of Analysis	☐ Engineering ☐ Performance Assessment ☒ Scientific
Intended Use of Analysis	☐ Input to Calculation ☐ Input to another Analysis or Model ☒ Input to Technical Document
Describe use:	

3. ☒ Model — Check all that apply

Type of Model	☒ Conceptual Model ☐ Abstraction Model ☐ Mathematical Model ☐ System Model ☐ Process Model
Intended Use of Model	☐ Input to Calculation ☐ Input to another Model or Analysis ☒ Input to Technical Document
Describe use:	
The intended use of this analysis and model is to determine the sensitivity of radionuclide transport to various input transport parameters.	

4. Title:

EBS Radionuclide Transport Model

5. Document Identifier (including Rev. No. and Change No., if applicable):

ANL-EBS-MD-000034 REV 00

6. Total Attachments:

5

7. Attachment Numbers - No. of Pages in Each:

I-5, II-5, III-3, IV-10, V-10

	Printed Name	Signature	Date
8. Originator	Katherine MacNeil	KM 04/13/00 ~~Signature~~ Katherine MacNeil	KM 04/13/00 ~~Date~~ 04/13/00
9. Checker	Veraun Chipman	John Peters for VC	4/13/00
10. Lead/Supervisor	Dwayne A. Chesnut	Dwayne A. Chesnut	04/13/2000
11. Responsible Manager	Dwayne A. Chesnut	Dwayne A. Chesnut	04/13/2000

12. Remarks:

John Case, Ernesto Faillace were primarily responsible for the development of this analysis (Section 6).

OFFICE OF CIVILIAN RADIOACTIVE WASTE MANAGEMENT
ANALYSIS/MODEL COVER SHEET
Complete Only Applicable Items

1. QA: QA

2. ☒ Analysis — Check all that apply

Type of Analysis	☐ Engineering ☐ Performance Assessment ☒ Scientific
Intended Use of Analysis	☐ Input to Calculation ☐ Input to another Analysis or Model ☒ Input to Technical Document
Describe use:	

3. ☒ Model — Check all that apply

Type of Model	☒ Conceptual Model ☐ Abstraction Model ☐ Mathematical Model ☐ System Model ☐ Process Model
Intended Use of Model	☐ Input to Calculation ☐ Input to another Model or Analysis ☒ Input to Technical Document
Describe use:	
The intended use of this analysis and model is to determine the sensitivity of radionuclide transport to various input transport parameters.	

4. Title:

EBS Radionuclide Transport Model

5. Document Identifier (including Rev. No. and Change No., if applicable):

ANL-EBS-MD-000034 REV 00

6. Total Attachments:	7. Attachment Numbers - No. of Pages in Each:
5	I-5, II-5, III-3, IV-10, V-10

	Printed Name	Signature	Date
8. Originator	Katherine MacNeil	KM 04/13/00 ~~Signature~~ Katherine MacNeil	KM 04/13/00 ~~Date~~ 04/13/00
9. Checker	Veraun Chipman	John Peters for VC	4/13/00
10. Lead/Supervisor	Dwayne A. Chesnut	Dwayne A. Chesnut	04/13/2000
11. Responsible Manager	Dwayne A. Chesnut	Dwayne A. Chesnut	04/13/2000

12. Remarks:

John Case, Ernesto Faillace were primarily responsible for the development of this analysis (Section 6).

OFFICE OF CIVILIAN RADIOACTIVE WASTE MANAGEMENT
ANALYSIS/MODEL REVISION RECORD

Complete Only Applicable Items

2. Analysis or Model Title:

EBS Radionuclide Transport Model

3. Document Identifier (including Rev. No. and Change No., if applicable):

ANL-EBS-MD-000034 REV 00

4. Revision/Change No.	5. Description of Revision/Change
00	Initial Issue

CONTENTS

FIGURES

Page

TABLES

ACRONYMS

ACC	Records Processing Center accession number
AFC	active fracture concept
AMR	analysis/model report
AP	administrative procedure
CRWMS M&O	Civilian Radioactive Waste Management System Management and Operating Contractor
DKM	dual permeability model
DOE	U.S. Department of Energy
DTN	data tracking number
EBS	Engineered Barrier System
EDA	enhanced design alternative
LADS	License Application Design Selection
LLNL	Lawrence Livermore National Laboratory
NBS	natural barrier system
NMR	Nuclear Magnetic Resonance
NUFT	Non-isothermal Unsaturated –saturated Flow and Transport
PMR	process model report
QA	quality assurance
QAP	quality administrative procedure
SAN	software activity number
SSC	Structures or components that have a high safety or waste isolation significance
STN	software tracking number
TBM	tunnel boring machine
TBV	to be verified
THC	Thermal-Hydrological-Chemical
THM	Thermal-Hydrological-Mechanical
TIC	Technical Information Center
Tptpll	Topopah Spring Tuff crystal poor lower lithophysal zone
Tptpmn	Topopah Spring Tuff crystal poor middle nonlithophysal zone
TSw2	Topopah Spring welded tuff
UFA	Unsaturated Flow Apparatus
UZ	unsaturated zone

NOMENCLATURE

C_l = Solute concentration of the solute at location x and time t (mg/l)
C_o= Solute concentration of the solute at location x =0 (mg/l)
D = Dispersion/Diffusion Coefficient (cm^2/sec) (De/θ)
D_e= Effective Dispersion/Diffusion Coefficient (cm^2/sec)
D_{lh} = Hydrodynamic dispersion coefficient (cm^2/sec)
D_n = Normalized dispersion coefficient (cm^2/sec)
D_{wl} = Binary diffusion coefficient (cm^2/sec)
D_{sl} = solute diffusion coefficient of solute in water (cm^2/sec)
D_s = Effective Solute Diffusion coefficient (cm^2/sec)
erf = Error function
erfc = Complementary error function
exp = Exponential function
G_s = Specific Gravity of Solids
i = counter for matrix or vector
j = counter for matrix or vector
J_{lh} = Diffusion flux (mm/yr)
J_w = Vertical flux rate (mm/yr)
K_d = Sorption coefficient (cc/gm)
L = Length in the vertical direction (cm)
Logt = Variable for graphing purposes
P_e = Peclet Number (V*L/D),
R = Retardation Factor
S_e= Saturation level
t = Time (sec)
Tr = Tortuosity
t_R = Dimensionless Time (v*t/L)
V = Pore Water Velocity (mm/yr)
z = Vertical Coordinate (m)
α_L= Dispersivity based upon Darcy Flux (cm)
β = Functional variable
ε = Integration variable
ϕ = Porosity
ψ = moisture potential (cm)
λ = Dispersivity based upon pore water velocity (cm)
ρ_s = Solid density (gm/cm^3)
θ = Volumetric moisture content
ξ (θ) = Liquid tortuosity factor

1. PURPOSE

The purpose of the Engineered Barrier System (EBS) radionuclide transport Analysis and Models Report (AMR) is to provide a description of radionuclide transport within the emplacement drift, as a result of releases from one or more breached waste packages.

A development plan (CRWMS M&O 2000a) was prepared in accordance with AP-2.13Q, *Technical Product Development Planning*. The plan documents this AMR number as E0050 and the corresponding work package as 1231213EM1. This report has been prepared according to this development plan and applicable quality assurance (QA) controls presented therein.

The intended use of this analysis and model is to determine the sensitivity of radionuclide transport to various input transport parameters. The model is not used for assessing post-closure system performance. It is a reasonably conservative one-dimensional model that solves the advective-dispersive-diffusive transport equation. The output described in the EBS *Water Distribution and Removal Model Input Transmittal* provide the flux and the volumetric moisture content to the one-dimensional contaminant transport equation. This equation is well known and widely accepted as the equation that describes radionuclide transport in porous media. Therefore, the confidence level is high for engineered, granular materials such as the invert, where this model will be applied. The one-dimensional contaminant transport equation will be used to generate breakthrough curves expressed as transport response to unit releases. As a minimum, the results of this analysis provide input data to the Engineered Barrier System Degradation, Flow and Transport Process Model Report (PMR).

1.1 BACKGROUND

The EBS radionuclide transport analysis is one of twenty-three Analysis/Model reports (AMRs) that support the development of the Engineered Barrier System Degradation, Flow and Transport Process Model Report. The EBS process model report (PMR) is part of a series of PMRs that have the general objective of documenting a synthesis of the necessary and sufficient technical information that the Project will be relying upon to support its site suitability evaluation and the licensing safety case pertaining to a particular process model. The technical information consists of data, analyses, models, software, and supporting documentation used to defend the applicability of the model for its intended purpose of evaluating the postclosure performance of the Yucca Mountain repository system.

EBS radionuclide transport through the invert represents one component of the overall EBS. Under some conditions, liquid water will seep into emplacement drifts through fractures in the host rock and move generally downward, potentially contacting waste packages. After waste packages are breached by corrosion, some of this seepage water will contact the waste, dissolve or suspend radionuclides, and ultimately carry radionuclides through the EBS to the near-field host rock.

Lateral diversion of liquid water within the drift will occur at the inner drift surface as a result of the performance of engineered structures such as drip shields, capillary barriers, and the outer surface of a penetrated waste package. If most of the seepage flux can be diverted laterally and

removed from the drifts before contacting waste package, the release of radionuclides from the EBS can be controlled, resulting in a proportional reduction in dose release at the accessible environment.

1.2 OBJECTIVES

The specific objectives of this model include:

- Generating contaminant transport breakthrough curves which express the transport response to unit concentration. Use of a one dimensional contaminant transport equation will provide a reasonable representation and bounding estimates for the time to breakthrough of radionuclides through the invert material. The effects of radioactivity will not be examined in the AMR because the breakthroughs for the long-lived radionuclides are rapid.

- Develop various scenarios for repository performance including:

  - Infiltration rate
  - Plugging of fractures below the EBS
  - Engineered features.

1.3 WORK SCOPE

A conceptual model of radionuclide transport through the emplacement drift and drainage features will be developed. The analysis may use, as available, information from the flow fields and fluxes from the EBS Water Distribution and Removal Model. The results of this analysis will include breakthrough curves in response to a unit concentration of RNs released from the WP.

1.3.1 Primary Tasks

- Identify design features and materials which describe the EBS radionuclide transport pathway.
- Identify environmental conditions and fluxes from the EBS Water Distribution and Removal Model.
- Develop conceptual models for EBS Radionuclide transport by advection and diffusion.
- Identify the inputs needed for model calculations and verify that input data are available in the Technical Data Management System.
- Analyze radionuclide transport by advection and diffusion.
- Perform sensitivity calculations.
- Discuss validation of the predictive model based on reasonably available data.

1.4 ANALYSIS/MODEL APPLICABILITY

The radionuclide transport results are applicable for the License Application Design Selection (LADS) repository configuration. General guidance on the selection of materials was provided by Wilkins and Heath (1999, Enclosure 2, p. 2) on the basis of thermal, hydrological, and geochemical consequences. The guidance included selection of a ballast material for the invert. Any significant change to these basic parameters would require an assessment of the subsequent impacts to this analysis/model.

2. QUALITY ASSURANCE

This document has been prepared according to AP-3.10Q, *Analyses and Models*. AP-3.10Q is the procedure for planning, developing, validating, and documenting analyses and models.

The applicability of the QA program is documented in an activity evaluation according to QAP-2-0, *Conduct of Activities*. The activity evaluation (CRWMS M&O 1999c) has concluded that this document is quality-affecting and subject to the QA controls of the *Quality Assurance Requirements and Description* (DOE 2000).

The design analysis, *Classification of the MGR Ex-Container System* (CRWMS M&O 1999a), was performed in accordance with QAP-2-3, *Classification of Permanent Items*. Radionuclide transport through the invert has been classified as QL-1. A QA classification of QL-1 refers to those systems, structures and components (SSCs) that have a high safety or waste isolation significance.

Qualified and accepted input data and references have been identified. Unqualified data used in this report are tracked in accordance with AP-3.15Q, *Managing Technical Product Inputs*. AP-3.10Q requires that output resulting from unqualified software be designated as unqualified—to be verified (TBV) in accordance with AP-3.15Q. Computer software and model usage is discussed in Section 3 of this report.

As per Section 5.9 of AP-3.10Q, the results of this analysis/model will be submitted to the Technical Data Management System in accordance with AP-SIII.3Q, *Submittal and Incorporation of Data to the Technical Data Management System*, if it is determined that the data developed in this document are needed by organizations outside of the Engineered Barrier Systems Operations organization.

3. COMPUTER SOFTWARE AND MODEL USAGE

Commercial software was used and is documented in accordance with AP-SI.1Q.

3.1 DESCRIPTION OF SOFTWARE USED

Crystal Ball, Version 4.0e is an add-in program for *Microsoft Excel.97*. It meets the definition of a software routine per Section 3.2.1 of AP-SI.1Q since it is a set of macros incorporated into a spreadsheet application that operates within another program (*Excel*). It is used to perform the uncertainty/sensitivity analysis on the input parameters described in Section 6.2.3. The single-use validation of only those portions of *Crystal Ball* used in this analysis is performed in accordance with AP-SI.1Q and is presented in Attachment V.

Microsoft Excel 97 is a commercial spreadsheet program designed to assist in routine calculations. The program provides built-in mathematical functions together with user-defined formulas to automate the calculation process. Output formulas are automatically updated as input data are added or changed. *Excel* also includes a graphical package to assist in data presentation. *Excel* was used in the calculation of the one-dimensional contaminant transport equation.

Mathcad 7Professional is an all-purpose program for performing and documenting mathematical calculations. *Mathcad* has many built-in functions for conducting mathematical calculations. *Mathcad* was used to calculate water flow rate through the invert and to generate the contaminant transport breakthrough curves. The single use validation of only those portions of *Mathcad* used in this analysis is performed in accordance with AP-SI.1Q and is presented in Attachment IV.

4. INPUTS

4.1 DATA AND PARAMETERS

4.1.1 Physical Parameters of the Invert Material

The physical parameters of the crushed tuff invert include the path length/distance, the invert porosity, and the grain density that are used in subsequent sensitivity analyses (Section 6.3). These are discussed below.

4.1.1.1 Path Length/Distance (m)

Path length/Distance (m) is defined as the thickness of the invert material. The thickness of the invert directly below the waste package is 0.606 meters (DTN: SN9908T0872799.004, file indriftgeom_rev01.doc). A rounded value of 0.61, for the thickness of the invert material, is used in Attachment I.

4.1.1.2 Dry Bulk Density and Porosity of the Invert Material

Porosity is the fractional volume in the invert material occupied by fluids (air or water). The reference invert fill material is assumed to be crushed tuff based on the assumption in section 5.10. The U.S. Geological Survey measured the bulk density, water retention, and unsaturated hydraulic conductivity measured using the UFA (DTN: GS980808312242.015). For materials sieved between 2.00 and 4.75 mm, used for hydraulic conductivity measurements, the dry bulk density was 1.15 g/cm^3 (DTN: GS980808312242.015). The data are currently qualified, Verification level 2. They are not related to the principal factors for the post-closure safety case identified in Attachment 6 of the AP-3.15Q. The *Water Diversion Model* (CRWMS M&O 2000e, p.23) developed the porosity as 0.545 for this material. The data is currently unqualified.

4.1.1.3 Grain Density

The grain density (g/cm^3) is the density of the solid matrix that makes up the invert material; it is not the bulk density, which takes into account the porosity. The estimated grain density equals 2.53 g/cm^3 (DTN: SN9908T0872799.004, file indriftgeom_rev01.doc). The data is currently unqualified. The *Cross Drift Geotechnical Predictive Report: Geotechnical Data Report* (CRWMS M&O 1998a, p.31) presents a range of saturated densities, and porosities for the Tptpll lithologic unit. The porosity of the Tptpll lithologic unit ranged from 0.088 to 0.176 based upon 21 measurements. The saturated bulk density ranged from 2.26 gm/cm^3 to 2.42 gm/cm^3 based upon these same measurements. An analysis of this data suggests a range in grain or solid densities from 2.49 gm/cm^3 to 2.72 gm/cm^3 (DTN: SNL02030193001.027). These data are currently qualified, Verification level 2. These data are not related to the principal factors for the post-closure safety case identified in Attachment 6 of the AP-3.15Q.

4.1.2 Hydrological Parameters of the Invert Material

The hydrological parameters of the invert material include the Darcy Flux rate, saturation levels the pore water velocities, and diffusion coefficients. The *Water Distribution and Removal Model*

Input Transmittal (CRWMS M&O 2000d, Item 1, pp.69,70) presents the saturation levels and pore water velocities for both uniform and focused glacial and present day infiltration rates with and without the benefits of the sand drain EBS drainage feature. Although the sand drain feature is not included in the LADS EDA II repository configuration, it was included in the parametric studies described in the *Water Distribution and Removal Model Input Transmittal* because they may create conditions in the emplacement drift where radionuclide transport is dominated by the mechanism of diffusion.

4.1.2.1 Volumetric Moisture Content

Volumetric moisture content is the fractional volume in the invert material occupied by water. It will be less than or equal to the porosity. From the saturation (S_e) results described in the *Water Distribution and Removal Model Input Transmittal* (CRWMS M&O 2000d, Item 1, p.70) presented in Table 1, the volumetric moisture content was determined to be 0.071 for the glacial climate, and present day with the exception of cases 9 and 10 (DTN: MO0003SEPRWDRM.001). For drier conditions that might result from a lower percolation rate 0.001 m/yr, the volumetric moisture content might equal the residual moisture content of 0.05 as determined in the *Water Diversion Model* (CRWMS M&O 2000e, p.23) based upon the multiplication of the invert residual liquid saturation of 0.092 (DTN: SN9908T0872799.004, file indriftgeom_rev01.doc) and the invert porosity of 0.545 (DTN: SN9908T0872799.004, file indriftgeom_rev01.doc).

Table 1. Saturation Levels and Volumetric Moisture Content

Case No.	Average Saturation Levels	Average Volumetric Moisture Content	Infiltration	Sand Drain
1	0.13	0.071	Glacial	No
2	0.13	0.071	Glacial	No
3	0.13	0.071	Glacial	No
4	0.13	0.071	Glacial	No
9	0.12	0.066	Glacial	Yes
10	0.12	0.066	Glacial	Yes
11	0.13	0.071	Present Day	No
12	0.13	0.071	Present Day	No
13	0.13	0.071	Present Day	Yes

Note: Refer to Table 13 described in the *Water Distribution and Removal Model Input Transmittal* (CRWMS M&O 2000d, Item 1, p.49) for a description of the parametric cases. The data are not qualified.

4.1.2.2 Pore Water Velocity

The pore water velocity is calculated as the Darcy Flux divided by the volumetric moisture content. Table 2 presents the pore water velocities in the invert (CRWMS M&O 2000d, p.69) (DTN: MO0003SEPRWDRM.001).

Table 2. Average Pore Water Velocity in the Invert

Case No.	Average Pore Water Velocity along the Center Line (mm/yr)	Average Pore Water Velocity along the Second Column (mm/yr)	Infiltration	Sand Drain
1	31	74	Glacial	No
2	33	77	Glacial	No
3	33	77	Glacial	No
4	32	75	Glacial	No
9	4.6E-02	4.6E-02	Glacial	Yes
10	4.6E-02	4.6E-02	Glacial	Yes
11	10	20	Present Day	No
12	10	22	Present Day	No
13	1.3E-02	NC	Present Day	Yes

Note: Refer to Table 13 described in the *Water Distribution and Removal Model Input Transmittal* (CRWMS M&O 2000d, Item 1, p.49) for a description of the parametric cases. The data is currently unqualified.

4.2 CRITERIA

There are no criteria applicable to the EBS Radionuclide Transport Model.

4.3 CODES AND STANDARDS

There are no codes and standards applicable to the EBS Radionuclide Transport Model.

5. ASSUMPTIONS

The following assumptions have been used in this EBS radionuclide transport model.

5.1 DIRECTION OF ADVECTIVE TRANSPORT

Advective transport in the invert occurs in the vertical direction at constant flux rates stated in the *Water Distribution and Removal Model Input Transmittal* (CRWMS M & O 2000d, Item 1, p.68) design for the glacial and present day climates. The present day climate is a relatively dry climate. However, because glacial climates dominated globally over the last million years, the glacial climate is considered. The glacial climate represents periods of extreme wetness and is therefore considered to provide a more conservative bounding analysis. This assumption is used in Section 6.2.2.

5.2 EFFECTS OF TRANSVERSE DISPERSION NEGLECTED

The effects of transverse dispersion are neglected in the analysis. Only longitudinal dispersion is considered in the analysis. This is a conservative assumption for analyzing breakthrough because transverse dispersion results in a lateral dispersion perpendicular to the direction of flow. This assumption is used in Section 6.2.2.

5.3 TRAVEL TIME OF CONTAMINANTS THROUGH HOMOGENEOUS INVERT MATERIAL

The technical basis for determining the shortest travel time of contaminants through homogeneous invert material relies on the phenomena that solutes in stream tubes of different velocity to mix (by diffusion or transverse dispersion) have a shorter time along a direction normal to the direction of mean convection than solutes moving through homogenous invert material by mean convection (Jury et al., 1991, page 221). This assumption is used in Section 6.2.2.

5.4 RADIONUCLIDE CONCENTRATION RELEASED OVER TIME IS CONSTANT

The concentration of radionuclides released from the waste package is considered to be constant over time, thereby making it more convenient to calculate the travel time with analytical solutions. This provides the technical basis for this assumption used in Section 6.2.2.

5.5 THE EFFECTS OF RADIOACTIVE DECAY IS NEGLECTED

The effects of radioactive decay is neglected. Therefore, contaminant breakthrough will occur rapidly relative to the half-life of long-lived radionuclides. This is a conservative assumption for analyzing time to breakthrough. This assumption is used in Section 6.2.2.

5.6 TEMPERATURE EFFECTS ON MOLECULAR DIFFUSION COEFFICIENT OF WATER ARE NEGLECTED

Temperature effects on the molecular diffusion coefficient of water are neglected in this AMR because the emplacement drift environment will be at near ambient temperature when the first waste package breaches after drip shield failure *Waste Package Degradation Process Model Report* (CRWMS M&O 2000c, p.3-121, Figure 3-83).

The solute diffusion coefficient (D_{sl}) is calculated on the basis of Archie's Law that modifies the binary diffusion coefficient of water/molecular diffusion of water (D_{wl}). The self diffusion coefficients of tritiated water (Mills 1973, p.685) in normal and heavy water were measured over a temperature range from 1°C to 45°C using the diaphragm-cell technique. These coefficients have been tabulated at various temperatures with an accounting of the molecular mass for water. These measurements were compared with the molecular dynamics and Nuclear Magnetic Resonance (NMR) data. The measurements show temperature dependence from 1.1×10^{-5} to 3.6×10^{-5} cm^2/sec (0.035 to 0.11 m^2/y) for 1°C and 45°C, respectively. Recent NMR studies were quoted and showed values at different temperatures that were in reasonable agreement with measurements by Mills (1973 pp. 687 to 688). Fetter (1993, page 44) states that the values for molecular diffusion or binary diffusion coefficient are well known, and fall in the range of from $1x10^{-5}$ to $2x10^{-5}$ cm^2/sec. Based upon Mills (1973 pp.687 to 688), a reasonable bounding value of $2.30x10^{-5}$ cm^2/sec or 0.073 m^2/y for the molecular diffusion coefficient of water at 25°C is used. Correcting the molecular diffusion coefficient of water for temperature is not expected to have a significant impact on the time to breakthrough when advection is the dominant mechanism of radionuclide transport through the invert (e.g after drip shield failure). In addition, greater uncertainty exists with the parameters that are of greater significance to radionuclide transport (e.g. volumetric moisture content, and Darcy flux) than the molecular diffusion coefficient for water. For example, the molecular diffusion coefficient for water at 45°C is only approximately 3 times greater than the value at 1°C (Mills 1973, pp.687-688).

The technical basis for this assumption is that the emplacement drift environment will be at near ambient temperatures when the first waste package breaches. Therefore selecting the molecular diffusion coefficient for water at 25°C provides a reasonable bound. This assumption is used in Section 6.2.2.

5.7 SOLUTE VAPOR PHASE IS NEGLIGIBLE

Solute vapor phase is negligible for the invert material. The technical basis for this assumption is that while it is possible for contaminants to be transported by vapor diffusion, the critical radionuclides from the standpoint of individual release are not volatile, but soluble in water, and can only be carried in the liquid phase. This is a bounding assumption. This assumption is used in Section 6.2.2.

5.8 NON-SORBING SOLUTES

Solutes do not react nor adsorb in the invert material. The technical basis for this assumption is that it is a conservative or bounding assumption since the effects of sorption as discussed subsequently is to increase retardation. This assumption is used in Section 6.2.2.

5.9 DISPERSIVITY

Dispersivity (m) is the degree of kinematic dispersion in the porous medium. Fetter provides a relationship dispersivity to length in Figure 2.18 of Fetter (1993, p.44). This figure shows that a conservative estimate of dispersivity for path length, expressed in Fetter (1993, p.44) as length (L), of one meter would be about 10 cm. Jury et al. (1991, p.222) discusses a range from 0.5 to 2 cm for packed laboratory columns, and from 5 to 20 cm in field experiments. Jury et al. (1991, p.222) state that the dispersivity can be considerably larger for regional groundwater flow; however due to the scale of the invert, these values would not apply. Based upon information provided by Jury et al. (1991, p.222), and Fetter (1993, p.44) a reasonable range of values would be from 0.4 to 10 cm. This assumption is used in Sections 6.1.1, 6.2.2, 6.2.3, 7.3, and IV-4. This assumption requires confirmation.

5.10 INVERT MATERIAL

The crushed tuff as the invert material was selected by Engineered Barrier System Operations so that Performance Assessment Operations could perform the TSPA-SR. CRWMS M&O 1999d, Item 2 discusses crushed tuff as the invert material. The crushed tuff is from the Tptpll lithostratigraphic unit, which is part of the TSw2 thermal/mechanical unit (CRWMS M&O 1997, p. 23). The Repository Host Horizon is located mainly in the TSw2 unit. The invert material hydrological properties are presently unavailable for the Tptpll formation. Properties for Tptpmn are used in this analysis. It is valid to substitute the Tptpmn properties in place of Tptpll values because they are both part of the TSw2 thermal/mechanical unit (CRMWS M&O 1997, p. 23). This assumption is used throughout. This assumption requires laboratory testing for confirmation.

5.11 PATH LENGTH RANGE

The range in path length in the invert varies from 0.5 to 0.7 m. The path length range will be used in the Monte Carlo Simulation calculations for the uncertainty and sensitivity analysis. The technical basis for this assumption is that the introduction of radionuclides might occur randomly beneath the waste package resulting in different path lengths. This assumption is used in Section 6.3.3.

5.12 PARTITION COEFFICIENT RANGE

The partition coefficient (K_d) is the ratio of the mass of solute (radionuclide) (g) adsorbed per mass of sorbent (invert material) (g) divided by the mass of solute (g) per volume of solution (H_2O) (mL). The partition coefficient is the function of the invert material as well as

electrochemical properties of the water and dissolved material. Monte Carlo Simulation calculations for the uncertainty and sensitivity analysis are performed for 5 ranges of distribution coefficients, each assuming a uniform distribution. The selected ranges are 0-1, 1-5, 5-10, 10-50, and 50-100 cm^3/g. The means are assumed to be at the midpoint of these distributions: 0.5, 3, 7.5, 30, 75 cm^3/g, respectively. This assumption is used in Section 6.3.3.

5.13 PARAMETERS USED IN MONTE CARLO SIMULATION ARE UNCORRELATED

The parameters used in the Monte Carlo Simulation are assumed to be uncorrelated. The technical basis for this assumption is that the eight parameters with the exception of the volumetric moisture content, and the Darcy Flux represent independent processes. For the case of these two parameters, the Darcy Flux and volumetric moisture content would depend directly on the percolation rate that would vary at the repository horizon. However, the volumetric moisture content would be near the residual moisture content as described in the *Water Distribution and Removal Model Input Transmittal* (CRWMS M&O 2000d, Item 1, p.38). For purposes of this analysis, it is reasonable to assume that these parameters are independent. This assumption is used in 6.3.3.

5.14 RANGE OF INVERT MATERIAL POROSITIES

The *Water Diversion Model* (CRWMS M&O 2000e, p.23) developed the porosity as 0.545 for this material. To estimate the range of porosities, it is noted that the density is high when the material is completely dry or saturated and low when the material has intermediate saturation (Fang 1991, p.261). The explanation for this phenomenon of bulking of sands is that small capillary stresses in the partly saturated material tend to resist the compressive stresses that occur due to compactive effort. The value presented above would represent the maximum porosity. Fang (1991 p.262) present information on the compactibility of cohesionless materials. For poorly graded sand a minimum porosity is estimated to be 0.28. This assumption is used in Section 6.2.3.

5.15 RANGE OF DARCY FLUX THROUGH THE INVERT MATERIAL

Darcy Flux (m/yr) is the volumetric flux of water through the center of the invert material. The Darcy Flux is determined from the mass flux rate described in the *Water Distribution and Removal Model Input Transmittal* (CRWMS M&O 2000d, Item 1, p.53) for various cases. The percolation rate in the surrounding rock varies as a function of location. A map of the percolation rate has been developed at the repository horizon (Section 4.1.2.1). Based upon the range of percolation rates at the repository horizon, the Darcy Flux range is from 0.001 to 0.0042 m/yr. A lower bound of 0.001 m/yr is selected. An upper bound of 0.0042 m/yr is selected which approximates twice the Darcy Flux in the invert (0.0022 m/yr), which is presented in Table 5. This bounding assumption is used in Section 6.2.3 and used in the sensitivity analysis presented in Attachment III.

6. ANALYSIS/MODEL

6.1 CONCEPTUAL MODEL DESCRIPTION

6.1.1 Conceptual Model Development for Engineered Barrier System Radionuclide Transport Model Description

The EBS Radionuclide Transport Model is a contaminant transport model within the invert below the waste package. One of the purposes of the EBS is to divert water flow to the invert before contacting the waste packages. A conceptual model was developed in the *Water Distribution and Removal Model* (CRWMS M&O 2000d, p.35) for how water is diverted in the EBS. As water enters the drift and flows through the backfill, the water flow will be diverted to (1) water flow through the drip shield that contacts the waste packages; (2) water flow that flows through the backfill directly to the invert; and (3) water flow that contacts the drip shield but does not flow through the drip shield.

Water that flows through the drip shield may contact the waste packages, and coalesce with water flow from the drip shield, and the backfill. The release of radionuclides from the Waste Package will result in a time dependent concentration of radionuclides that in this conceptual model is considered a unit concentration (Figure1). Note that in a steady state flow field where pore velocities and volumetric moisture content are not changing with time, the contaminant transport equation is linear. The principle of superposition is then used in the model to obtain a solution to the problem where the inlet concentration is varying with time.

If the transport of radionuclides through the invert were dominated by diffusion then the time to breakthrough of radionuclides would increase compared to the breakthrough time for advection dominated transport. The diffusive barrier materials emplaced (crushed tuff) are considered to be non-sorbing and sorption mechanisms are excluded as discussed previously in Section 5.7.

The one-dimensional advection/dispersion/diffusion equation (Jury et al. 1991, p.223) is used to evaluate the effects of advection/dispersion/diffusion on radionuclide migration through a porous medium such as crushed tuff. The crushed tuff is evaluated as to its ability to increase the breakthrough time from the EBS, via transport dominated by molecular diffusion.

The following discussion describes how the advection/dispersion/diffusion equation is utilized to generate the contaminant breakthrough curves for the radionuclide transport model. The invert flow rates are determined in the *Water Distribution and Removal Model* (CRWMS M&O 2000d, p.68) and are used to calculate the volumetric moisture content and pore water velocities (average linear velocities) for the invert (crushed tuff) (Section 4.1.2.2). The above mentioned parameters are determined for the chimney L4C4 in the *Water Distribution and Removal Model* (CRWMS M&O 2000d, p.38). This chimney location is representative of the repository environment for two different climate conditions: the present day climate, and glacial climate, which are defined in the *Water Distribution and Removal Model* (CRWMS M&O 2000d, p.46).

In the advection/dispersion/diffusion contaminant transport equation for unsaturated flow, the diffusion coefficient becomes a function of the saturation or volumetric moisture content.

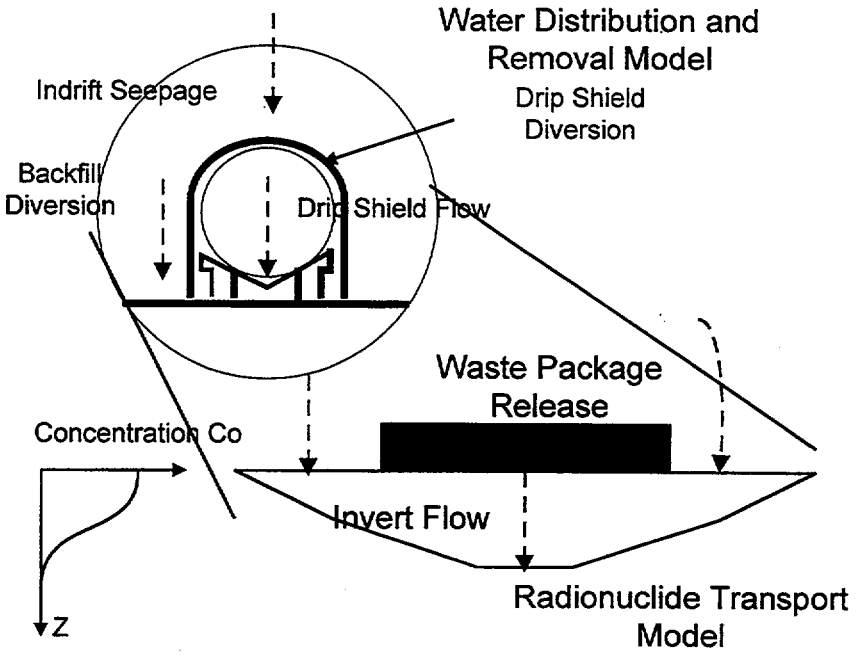

Figure 1. Conceptual Model for Radionuclide Transport

The diffusion coefficient for various radionuclides depends on the self diffusion of water (Section 5.6), and the volumetric moisture content for unsaturated flow through a porous media, and the mechanical mixing or hydrodynamic dispersion that is a function of the pore water velocity (Fetter 1993, p.185).

The tortuosity relation based upon Archie's Law from the *Invert Diffusion Properties Model* (CRWMS M&O 2000b, p.20), is used to determine the solute diffusion coefficient. The solute diffusion coefficient can be determined by multiplying the binary diffusion coefficient for water by the tortuosity factor. The hydrodynamic dispersion coefficient is determined by multiplying the pore water velocity by the dispersivity. A dispersivity of 10 cm is selected based on engineering judgement (Section 5.9), since, in the field, dispersivity ranges from 5-20 cm (Jury et al. 1991, p.222).

The ratio of the hydrodynamic dispersion coefficient to the solute diffusion coefficients are then determined (Fetter 1993, pp. 54-57). A ratio greater than one indicates that dispersion is dominant. The dispersion/diffusion coefficient for crushed tuff for application to the one-dimensional advection/dispersion/diffusion equation is calculated (Attachment IV) by dividing the effective dispersion/diffusion coefficient, which is the summation of the hydrodynamic dispersion coefficient and the solute diffusion coefficient by the mean volumetric moisture content.

6.1.2 Physical and Chemical Environment of the Invert and Adjacent Floor Rock

The physical chemical environment of the invert as applied to radionuclide transport in the absence of chemical retardation involves the liquid saturation levels in the invert, and how liquid

saturation levels are influenced by temperature and the evaporation rate. Saturation levels are also influenced by alterations in the fracture system directly below the invert due to Thermal-Hydrological-Chemical (THC), and Thermal-Hydrological-Mechanical (THM) effects. These effects are discussed below.

The condition of dryout (zero or low liquid saturation) is greater for low-flux conditions. Water returns to the EBS environment sooner for high-flux conditions and for repository-edge conditions.

During the repository excavation, the in situ state of stress is relieved, and the potential exists for movement to occur due to elastic or elastoplastic deformation (CRWMS M&O 2000d, p.36). The stress redistribution and Tunnel Boring Machine (TBM) excavation to form a modified permeability zone that depends upon the in situ state of stress, rock deformational and strength properties. Rock fines resulting during TBM excavation might also affect the drainage of the fractures. Further, during repository heating and cooling during the postclosure period, the potential exists for additional stress redistribution that would affect the retention and flow characteristics of the surrounding media. These combined effects result in alteration of the properties due to thermal and mechanical effects.

The effect of stress relief and dilation on fractures would tend to result in an increase in the saturated hydraulic conductivity with an attendant reduction in retention characteristics. These combined effects may result in a lowering of unsaturated hydraulic conductivity. Rock fines resulting from TBM excavation will reduce the saturated hydraulic conductivity while increasing the retention characteristics of the fractures.

Other coupled processes (Hardin 1998, p.2-3) during the thermal period may significantly alter hydrologic properties that influence refluxing and seepage. Because of mineral dissolution and precipitation reactions, and precipitation in response to the elevated temperature environment or evaporation, THC effects will cause alteration of flow paths above and below the repository emplacement drifts. When zones have no liquid outflow, substantial accumulation of soluble salts may occur from evaporation (the zones need not be dry for this to occur). For the "lower" infiltration results, there is greater potential for solute accumulation in the invert.

6.2 DETAILED MODEL DESCRIPTION

6.2.1 Engineered Barrier System Flow Rates Extracted from Water Distribution and Removal Model Results

In this section, the results of the NUFT calculations as they pertain to the invert are presented. These results establish the pore water velocity (V), and the saturation levels (S_e) or volumetric moisture content that is used in the radionuclide transport model. The NUFT calculations establish the flux rates through invert based upon the hydrologic performance of the drip shield, the backfill, the invert, and the surrounding host rock.

The results of the NUFT analysis for the *Water Distribution and Removal Model* (CRWMS M&O 2000d, pp.50-52) for the base case of focused flow at isothermal temperature are presented

in Figures 2 to 5. These analyses showed that a drip shield lobe (zone of increased flux rate) is evident from review of the base case. The downward mass flux rate that expresses the deflection sideways from the drip shield produced by the runoff of water unable to penetrate the drip shield is in qualitative agreement with the exclusion analysis for a circular cavity (Philip et al. 1989, p.25). The fluxes in the zone adjacent to the drip shield are increased by a factor of three to four with respect to far field flow.

Below the drip shield, the absolute value of the capillary pressure is increased from approximately 36,000 Pa (370 cm) to approximately 50,000 (510 cm). As predicted by the conspectus and exclusion analysis for cylindrical cavities (Philip et al. 1989, p. 21), a "dry shadow" forms below the drip shield in which the absolute value of the capillary pressure is increased and the saturation levels are reduced. The flow rates through the invert are presented in Table 3 (CRWMS M&O 2000d, Item 1, p.69).

In summary, the results from NUFT calculations show that for the invert that flux rates would be reduced below the drip shield, and increased through the invert outside the drip shield. The discussion presented subsequently (Section 6.3.1 to 6.3.2) presents the pore water velocities for the several cases, and vector plots that illustrate the direction and magnitude of water flux.

Table 3. Summary of Flow Rates through the Invert

Case No.	Flow Below the Drip Shield (m3/yr)	Flow Outside of the Drip Shield
1	0.16	0.25
2	0.17	0.26
3	0.17	0.25
4	0.17	0.26
5	-	-
6	-	-
7	-	-
8	-0.83	0.005
9	$1.6*10^{-5}$	0.36
10	$1.6*10^{-5}$	0.36

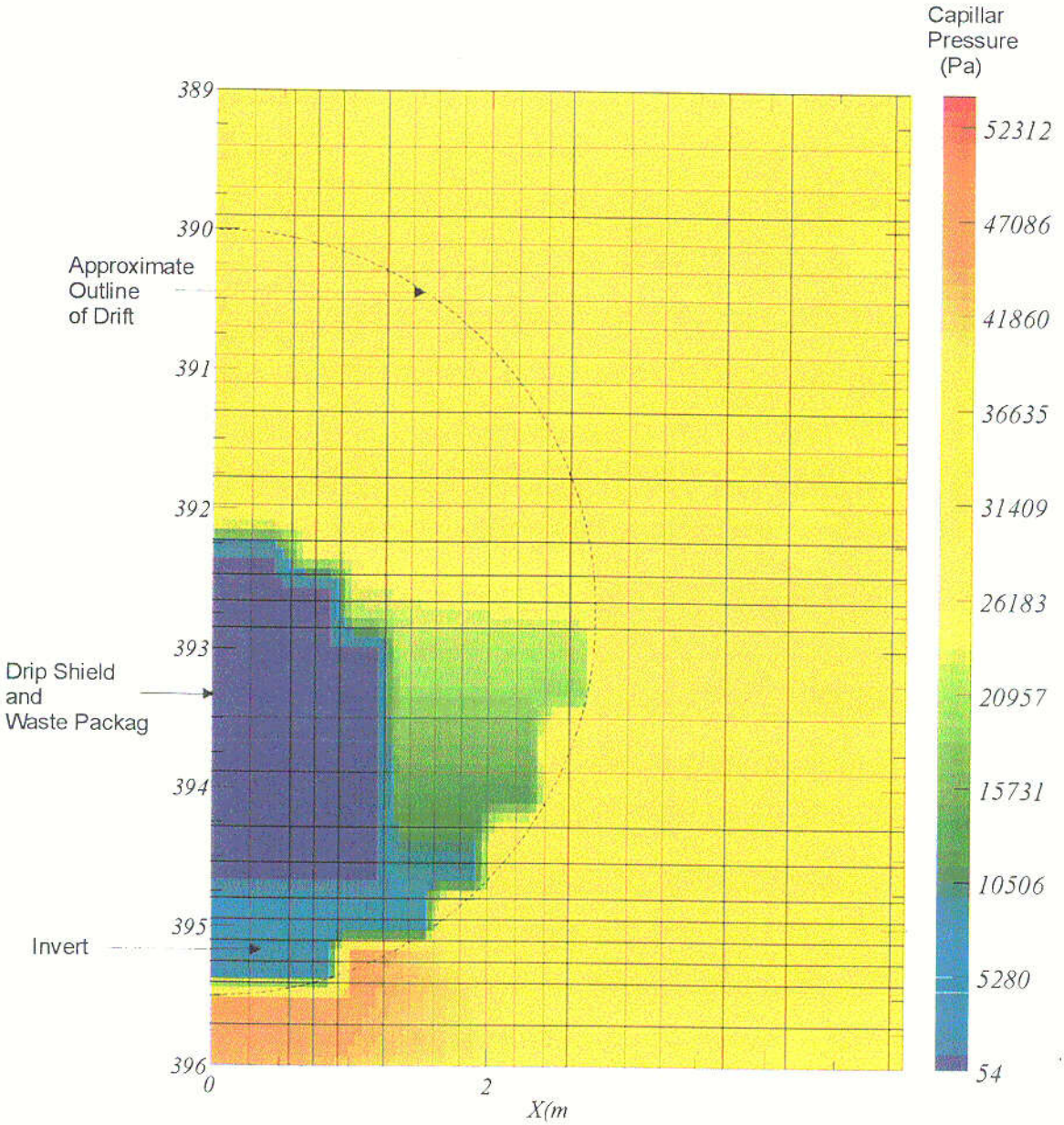

Figure 2. Absolute Matrix Capillary Pressure for Focused Flow at Steady State at Isothermal Temperature Near the Repository Horizon (Case 1)

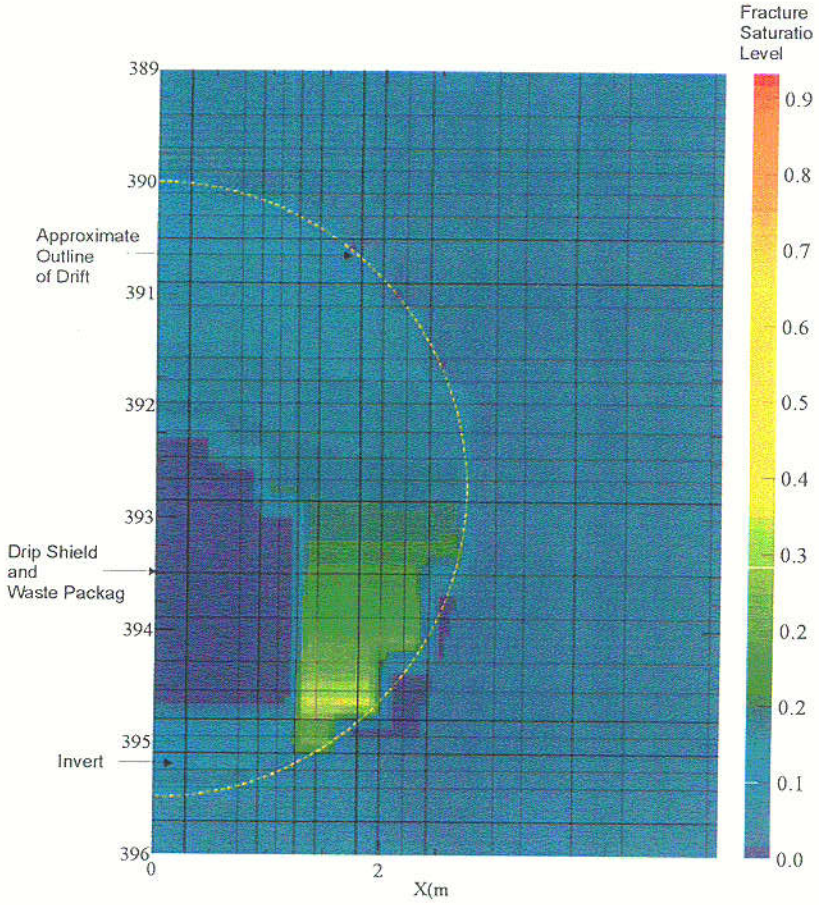

Figure 3. Fracture Saturation Levels for Focused Flow at Steady State at Isothermal Temperature Near the Repository Horizon (Case 1)

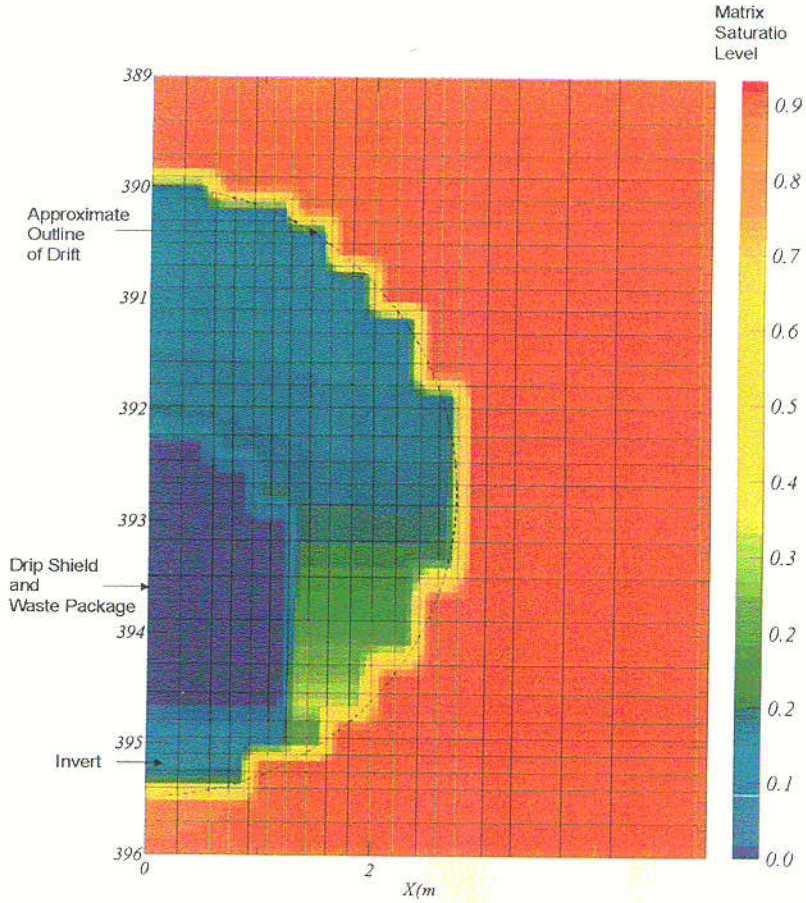

Figure 4. Matrix Saturation Levels for Focused Flow at Steady State at Isothermal Temperature Near the Repository Horizon (Case 1)

C2

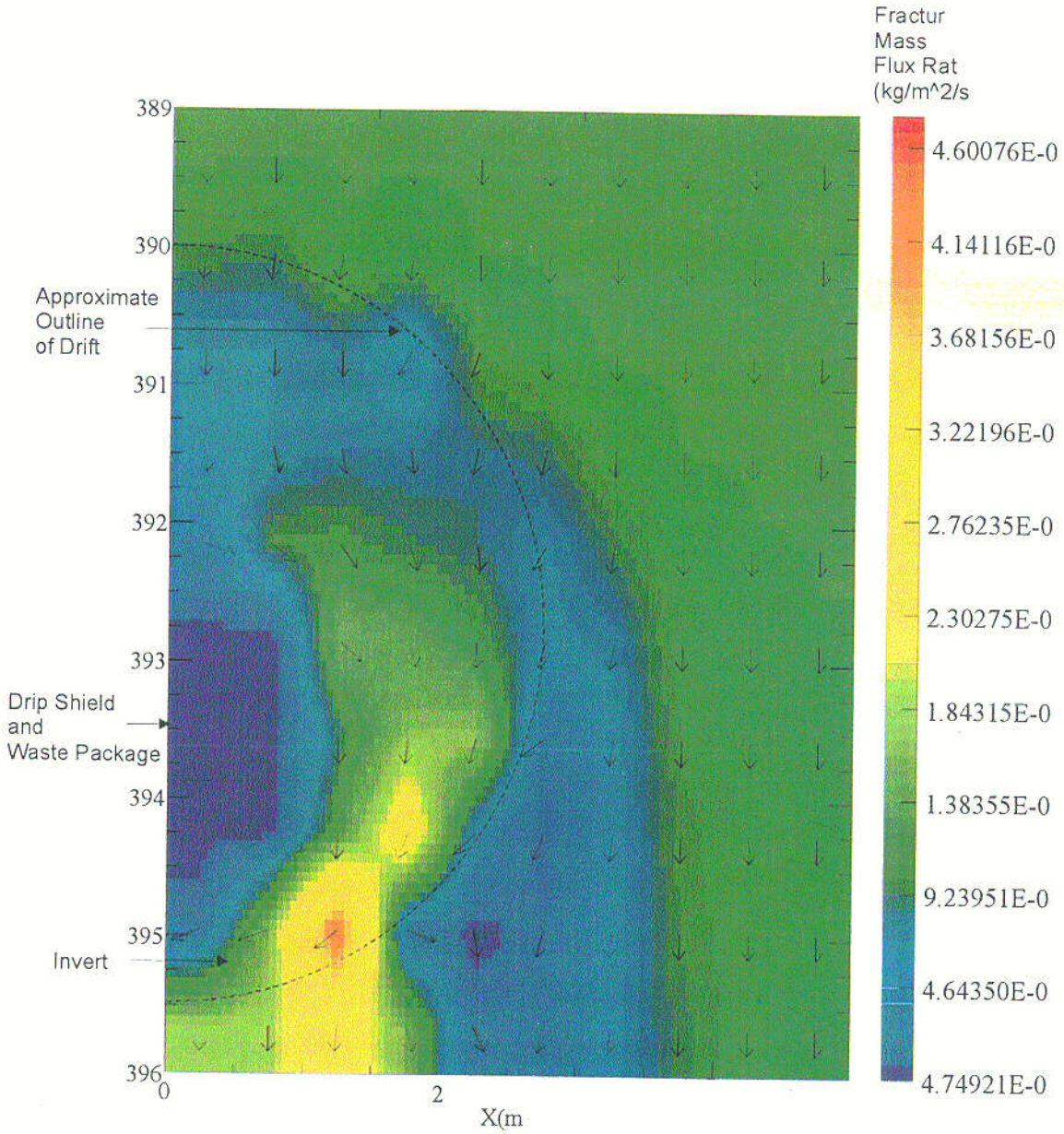

Note: mass flux rates within the drift are a factor two higher.

Figure 5. Fracture Mass Flux Rates (kg/m^2-s) and Direction of Flow for Focused Flow at Isothermal Temperature Near the Repository Horizon (Case 1)

6.2.2 Detailed Model Description

The simplest chemical transport processes in the invert are those that involve nonvolatile dissolved solutes that neither chemically react nor physically adsorb to the invert solids. The one dimensional advection-dispersion-diffusion relation for contaminant transport or breakthrough

for those solutes whose vapor phase is negligible (Section 5.7) and nonreactive (Section 5.8) is analyzed for by solving the equation (Jury et al. 1991, p. 222):

$$\frac{d}{dt}C_l = D \cdot \frac{d^2}{dz^2} C_l - V \cdot \frac{d}{dz} C_l \qquad \text{(Eq. 1)}$$

At t = 0, water is instantaneously introduced in the invert material and continues at a constant flux rate J_W in the vertical direction. The radionuclides are also introduced to the invert material at a concentration C_o at a continuous rate.

A solution to the above relation is presented by Freeze and Cherry (1979, page 391) for nonretarded transport in one dimension with initial concentration C_o at a continuous rate in which the vapor phase transport is negligible (Sections 5.2 to 5.5 and Sections 5.7 to 5.8):

$$\frac{C_l}{C_o} = \frac{1}{2} \cdot \left(\operatorname{erfc}\left(\frac{L - V \cdot t}{2 \cdot \sqrt{D \cdot t}} \right) + \exp\left(\frac{V \cdot L}{D} \right) \cdot \operatorname{erfc}\left(\frac{L + V \cdot t}{2 \cdot \sqrt{D \cdot t}} \right) \right) \qquad \text{(Eq. 2)}$$

The effective dispersion-diffusion coefficient can be derived as (Jury et al. 1991, page 222):

$$D_e = D_{lh} + D_{sl} \qquad \text{(Eq. 3)}$$

Further, the diffusion coefficient (D) equals the effective dispersion-diffusion coefficient (D_e) divided by the volumetric moisture content (θ) (Jury et al., 1991, p.223).

The solute hydrodynamic dispersion flux has a form that is mathematically identical to the diffusion flux (Jury et al. 1991, page 221):

$$J_{lh} = -D_{lh} \frac{d}{dz} C_l \qquad \text{(Eq. 4)}$$

This coefficient has frequently been observed to be proportional to the pore water velocity $V = J_W/\theta$ (Jury et al. 1991, page 221) (Section 5.9):

$$D_{lh} = \lambda \cdot V$$

(Eq. 5)

The solute diffusion coefficient (D_{sl}) is a function of the binary diffusion coefficient in water, and a function of $\xi(\theta)$ (Jury et al. 1991, page 221) which is a liquid tortuosity factor to account for the increased path length and decreased cross-sectional area of the diffusing solute in the invert.

The solute diffusion coefficient is given by (Jury et al. 1991, p.221) (Section 5.6):

$$D_{sl}(\theta) = \xi(\theta) D_{wl}$$

(Eq. 6)

The diffusion coefficient applies to crushed tuff that is assumed to comprise the invert (Section 5.10). In the *Invert Diffusion Properties Model* (CRMWS M&O 2000b, page 20 of 30), a collection of diffusion coefficients was evaluated, and the normalized diffusion coefficient (D_n) was given by:

$$D_n = \phi^{1.3} S_e^2$$

(Eq. 7)

This relationship can be expressed in terms of volumetric moisture content by substituting ϕS_e for the volumetric moisture (θ):

$$D_s = D_{wl} * \phi^{-0.7} \theta^2$$

(Eq. 8)

In the solution of the contaminant transport equation for porous media flow, de Marsily (1986, p. 267) writes the basic contaminant transport equation based upon the flow through the pore space that entails the porosity for saturated flow, and the Darcy Flux. The governing equation for contaminant transport is identical to the relation presented by Jury et al. (1991, p. 222); however the formulation for diffusion and dispersion for a saturated porous media is written as (de Marsily 1986, p. 238):

$$D = \phi * D_s + \alpha_l * J_w$$

(Eq. 9)

For unsaturated flow, the flow and diffusion-dispersion that occurs through the pore space is diminished by the degree of saturation. This is because in unsaturated flow, the occurrence or retention of water within the pore space is reduced as the soil becomes drier.

The above relation becomes upon the substitution of θ for ϕ:

$$D = \theta * D_s + \alpha_l * J_w \qquad \text{(Eq. 10)}$$

If Equation 8 is substituted into Equation 10, the following relationship is developed:

$$D = \theta * D_{lh} * \phi^{-0.7}\, \theta^2 + \alpha_l * J_w \qquad \text{(Eq. 11)}$$

A comparison of Equation 11 that is developed from basic relations presented by de Marsily (1986 p. 238) to the Equation 3 developed from relations presented by Jury (1991, p. 221) shows that the two relationships are identical if the tortuosity factor $\xi(\theta)$, and the dispersivity are defined differently. The dispersivity in the former case is based upon the Darcy flux J_w while in the latter case, it is based upon the porewater velocity V. Further the soil water diffusion is equivalent in the two formulations if the tortuosity factor presented by Jury 1991, p: 221 is selected as:

$$\xi(\theta) = \theta^3 \phi^{-0.7} \qquad \text{(Eq. 12)}$$

The relations in Equations (3), (5), (6) and (12) are used to calculate the effective diffusion-dispersion coefficient (D_e) for the diffusive barrier. The diffusion-dispersion coefficient (D) used in Equation (1) equals the effective diffusion-dispersion coefficient (D_e) for the diffusive barrier. The diffusion-dispersion coefficient (D) used in Equation (1) equals the effective diffusion-dispersion coefficient (D_e) divided by the volumetric moisture content (θ). After determining these properties, Equation (2) as presented in Attachments I to IV is used subsequently to calculate the breakthrough curve for the diffusive barrier for the case of no retardation.

A comparison can be made of the relationship of D_{sl} to volumetric water content (θ) for comparison to measured diffusion coefficients for crushed tuff (CRWMS M&O 1999d, Item 2, p. 12), and the modified form of the Millington Quirk relation (Jury et al. 1991, p.221) for D_{sl} with the use of the binary diffusion coefficient D_{wl} for water (Section 5.6). Figure 6 illustrates these comparisons and shows that at low volumetric moisture contents, the relationship based upon Archie's Law as developed in the *Invert Diffusion Properties Model* (CRWMS M&O 2000b, p.20) is comparable to the modified form of the Millington Quirk relation, and in approximate agreement with measured data for crushed tuff.

de Marsily (1986, p.233) presents a relationship between the molecular or binary diffusion coefficient, and soil-liquid diffusion coefficient D_s. For saturated conditions, the ratio of the soil-liquid diffusion coefficient to the molecular diffusion coefficient varies from 0.1 to 0.7 for sands.

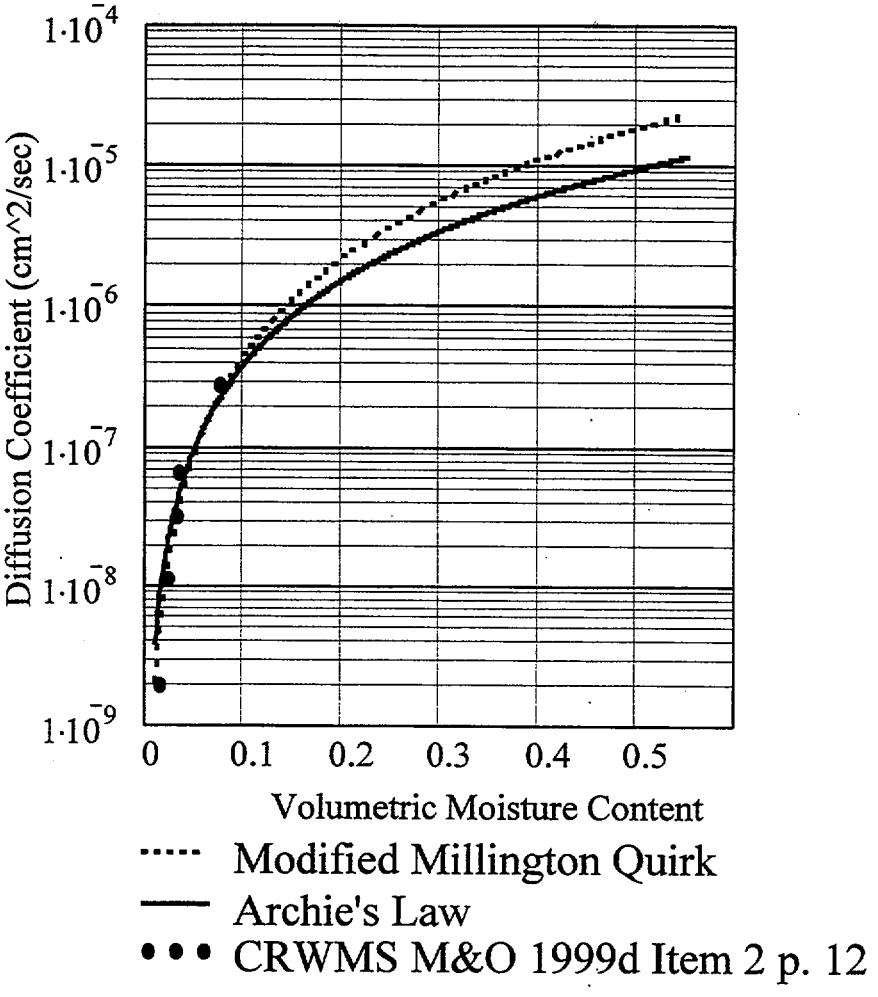

Figure 6. Comparison of Measured Data for Crushed Tuff with Archie's Law, and the Modified Millington Quirk Relation.

Note: Table 1 of CRWMS M&O 1999d, Item 2, p.12 presents diffusion coefficient data.

The calculated value from Equation 8 is 0.46 for a porosity for the invert (Section 4.1.1.2) of 0.545 from Archie's Law. This value falls within this range of values.

6.2.3 Radionuclide Transport Summary

The summary parameters and the range of parameters are for the physical, hydrological, and chemical parameters used in the model are presented in Table 4.

Table 4. Summary of Parameter Values and Ranges Used in The Analysis

Parameter Name, Units	Parameter Value	Source	Parameter Range	Source
Path Length/Distance (L) (m)	0.61	Section 4.1.1.1	0.5 - 0.7	Section 5.11
Volumetric Water Content (θ)	0.071	Section 4.1.2.1	0.05 - 0.07	Section 4.1.2.1
Pore Water Velocity (V) (m/yr)	0.031	Section 4.1.2.2	0.013 - 0.031	Section 4.1.2.2
Darcy Flux (J_w) (m/yr)	0.0022	*	0.001 - 0.0042	Section 5.15
Porosity (ϕ)	0.545	Section 4.1.1.2	0.28 - 0.55	Section 5.14
Dispersivity (α_l) (m)	0.1	Section 5.10	0.004 - 0.1	Section 5.10
Molecular Diffusion Coefficient (D_{wl}) (m^2/yr)	0.073	Section 5.6	0.035-0.11	Section 5.6
Grain Density (ρ_s) (g/cm^3)	2.53	Section 4.1.1.3	2.49 - 2.72	Section 4.1.1.3
Partition Coefficient (Kd) (cm^3/g)	0	Section 5.12	0-1, 1-5, 5-10, 10-50, 50-100	Section 5.12

* Note: The Darcy Flux value of 0.0022 m/yr is estimated by multiplying the pore water velocity for Case 1 (Section 4.1.2.2, Table 2) multiplied by the volumetric moisture content for Case 1 (Section 4.1.2.1, Table 1).

The one-dimensional solute transport equation may be solved with the input of the parameters listed in Table 4. When used in the uncertainty/sensitivity analysis, a distribution of the parameter values must be defined based on assumptions or data measurements. In addition, the bounds, means, and or standard deviations of the parameter distributions must be defined. For a more detailed discussion of the parameters and ranges listed in Table 4, which are used in the uncertainty/sensitivity analysis (Attachment III), refer to the appropriate sections in Sections 4.1 and 5.

6.3 EBS RADIONUCLIDE TRANSPORT RESULTS

6.3.1 Base Case for the Radionuclide Transport Model

The following discusses the base case for radionuclide transport through the invert. The base case is identified as Case 1 in Table 1. The pore water velocity V, and the volumetric moisture content θ occur under steady state conditions in the invert. These results described in the *Water Distribution and Removal Model* (CRWMS M&O 2000d, Item 1, pp.69,70) (Sections 4.1.2.1 - 4.1.2.2), are combined with other parameters characterizing diffusion, and the hydrodynamic dispersion for evaluation of the base case for radionuclide transport. Table 4 above presents these inputs.

A range of the percolation rate has been considered at the repository horizon and is described in the *Water Distribution and Removal Model Input Transmittal* (CRWMS M&O 2000d, Item 1). In the *Water Distribution and Removal Model Input Transmittal* (CRWMS M&O 2000d) the invert is subdivided into grid blocks for NUFT modeling. The removal of water in the invert reduces the flux and increases the groundwater travel time for plug flow in the invert. The mass

flux rate below the waste package for the base case is presented in the *Water Distribution and Removal Model* Input Transmittal (CRWMS M&O 2000d, Item 1, p.52, Figure 11). To obtain the Darcy flux (volumetric flux rate) for each grid block the mass flux rate is divided by the density of water (1.0 gm/cm^3) (CRWMS M&O 2000d, Item 1, p.53). A maximum percolation rate in the surrounding rock for the glacial climate was calculated as 42 mm per year and resulted in a Darcy flux rate of 2.2 mm per year in the invert. The volumetric moisture content in the invert (Table 1) is approximately 0.071.

The pore water velocity (V) (Jury et al., 1991, p. 222) is calculated as the Darcy flux (volumetric flux rate) (J_w) divided by the volumetric moisture content for each grid block. The saturation levels are used to estimate the pore water velocity from the flux rate, and the volumetric moisture content for each grid block. The travel time can be estimated for each grid block, and then added to obtain the total travel time from the top of the invert to the bottom of the invert (CRWMS M&O 2000d, p.69). The average pore water velocity of 31 mm per year can be calculated by dividing the path length of 0.61 m by the total travel time of approximately 20 years. Figures 7 and 8 present a plot of the matrix and fracture pore water velocities as obtained from the *Water Distribution and Removal Model Input Transmittal* (CRWMS M&O 2000d, p. 71). Note that within the invert away from the drift boundary, the velocity vectors are identical while for grid blocks near the boundary, the flow is dominantly into the fractures. The pore water velocity in the adjacent column of grid blocks is increased by an approximate factor of 2.4 (CRWMS M&O 2000d, p.69).

The radionuclide breakthrough curve as calculated from Equation 2 for the base case is presented in Figure 9. The results show that the breakthrough is substantial after 10 years, and is nearly complete after 100 years. Also, the analysis shows that for areas adjacent to the centerline of the invert breakthrough occurs more rapidly. As the distance increases from the centerline, pore water velocities in the vertical direction become larger with breakthrough occurring sooner.

The calculated values for solute (soil-liquid) diffusion (D_{sl}) of $1.25*10^{-6}$ cm^2/sec, and hydrodynamic dispersion (D_{lh}) $9.82*10^{-7}$ cm^2/sec (Attachment IV-5) are of comparable magnitude for the input parameters in Table 4. While the analysis shows that there is a reduction in flux rates within the invert due to the formation of a dry shadow below the drip shield, it also shows that for the input parameters used in this analysis (Table 4), that the porewater velocity is sufficiently high that hydrodynamic dispersion is significant.

6.3.2 Sensitivity of Calculated NUFT Results to Coupled Thermal-Hydrological-Chemical Processes in the Engineered Barrier System

Table 2 presents the pore water velocity at the centerline of the emplacement drift for other cases, and in an adjacent column for comparison to the base case described in the *Water Distribution and Removal Model Input Transmittal.* The other cases considered the effects of uniform versus focused flow and the effects of heating. Also, the other cases considered the effects of fracture plugging, and the performance of sand drains. These analyses found that the effects of repository heating were not significant. The results showed that the plugging of fractures would increase invert saturation while the installation of sand drains would increase travel time, and reduce pore water velocity.

Sand drains are not part of the LADS EDA II repository configuration. It is important to discuss sand drains because they may create conditions in the emplacement drift where radionuclide transport is dominated by the mechanism of diffusion. Consider the case of a sand drain (Case No. 9). In this case the fractures are plugged, and a sand drain is provided with material with unsaturated flow properties identical to the backfill. The breakthrough time for plug flow through a length of 0.6 m is estimated to be 47,000 years for the present day climate, and 13,000 years for the glacial climate. The breakthrough times for plug flow for the case of the sand drain are three orders of magnitude higher than the base case. The presence of the sand drain for the case of glacial infiltration reduces advective transport through the invert, and increases the likelihood of the invert to act as a diffusion barrier. The pore water velocity vectors for this case are shown in Figures 10 and 11 for the fracture and matrix components respectively, show that dominant drainage occurs vertically downward through the sand drain for this case. In contrast, the base case or Case No. 1 reflects a flow pattern in which flow exclusion takes place due to the drip shield. For the base case, there is a horizontal component of flow below the drip shield (Figures 7 and 8) while this component of flow is not apparent in the case of the sand drain.

The radionuclide breakthrough curve for the case of sand drains for comparison to the base case as calculated from Equation 2 is presented in Figure 12. The results show that breakthrough is substantially delayed. Also, the analysis shows that for areas adjacent to the centerline of the invert breakthrough is also substantially delayed.

The breakthrough for the present day climate are presented in Figure 13. The percolation rate at the repository horizon is smaller resulting in somewhat increased groundwater travel times and lower pore water velocities in the invert. The results show that breakthrough is substantial after 10 years, and nearly complete after 100 years.

The effects of the sand drains for the present day climate are presented in Figure 14. The figure presents the breakthrough curve for the case of no drains for comparison. The analysis shows that as in the case of the glacial climate that breakthrough is substantially delayed.

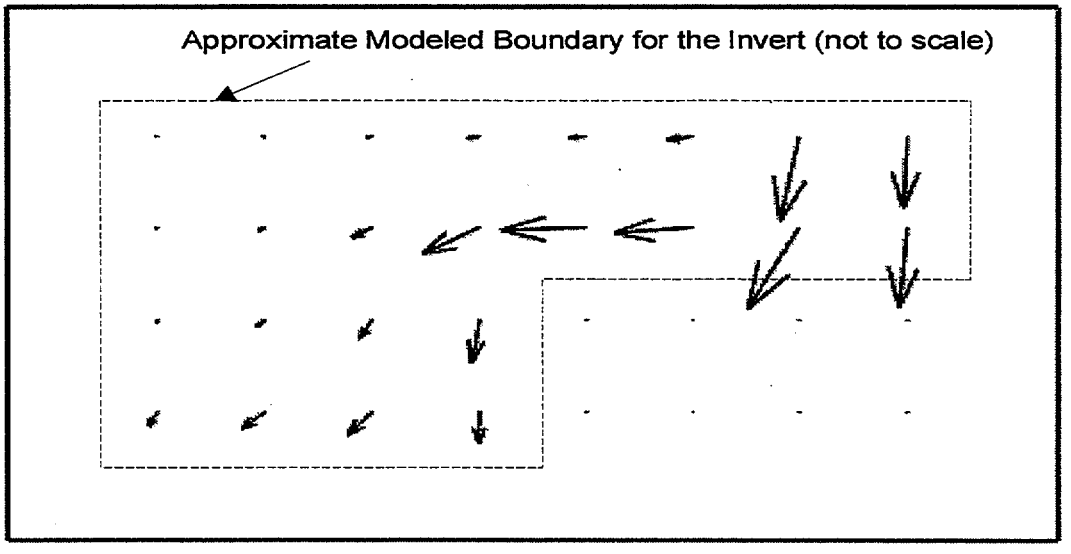

Figure 7. Fracture Pore Water Velocity Vectors in the Invert for the Base Case

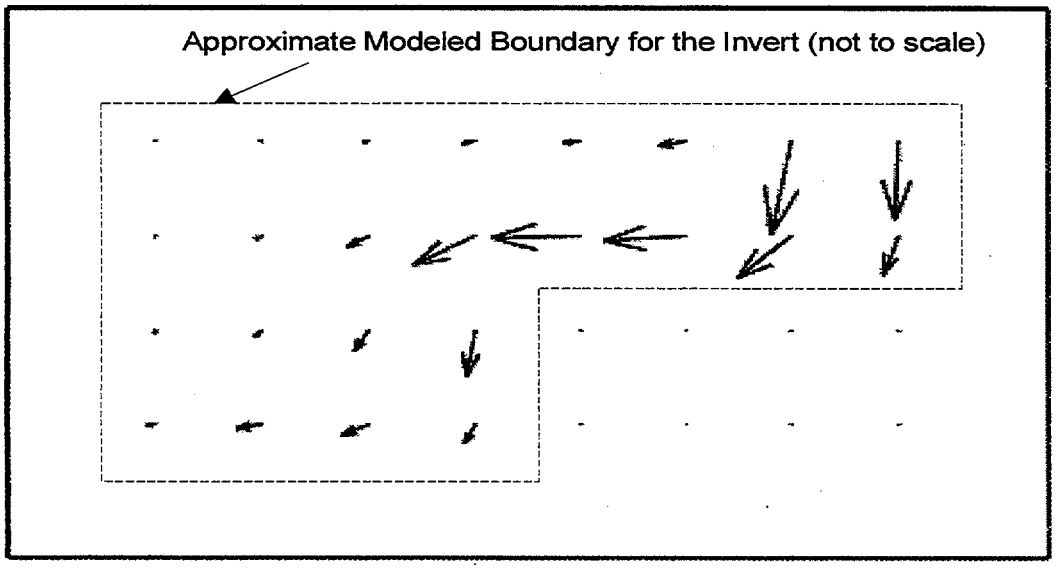

Figure 8. Matrix Pore Water Velocity Vectors in the Invert for the Base Case

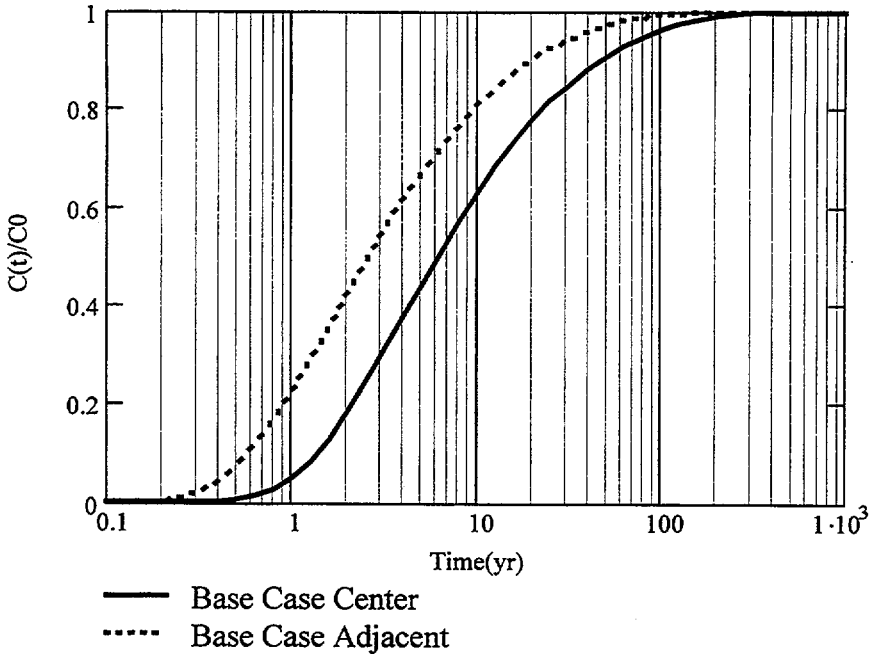

Figure 9. Breakthrough for One Dimensional Advection/Dispersion/Diffusion for the Base Case (Case 1)

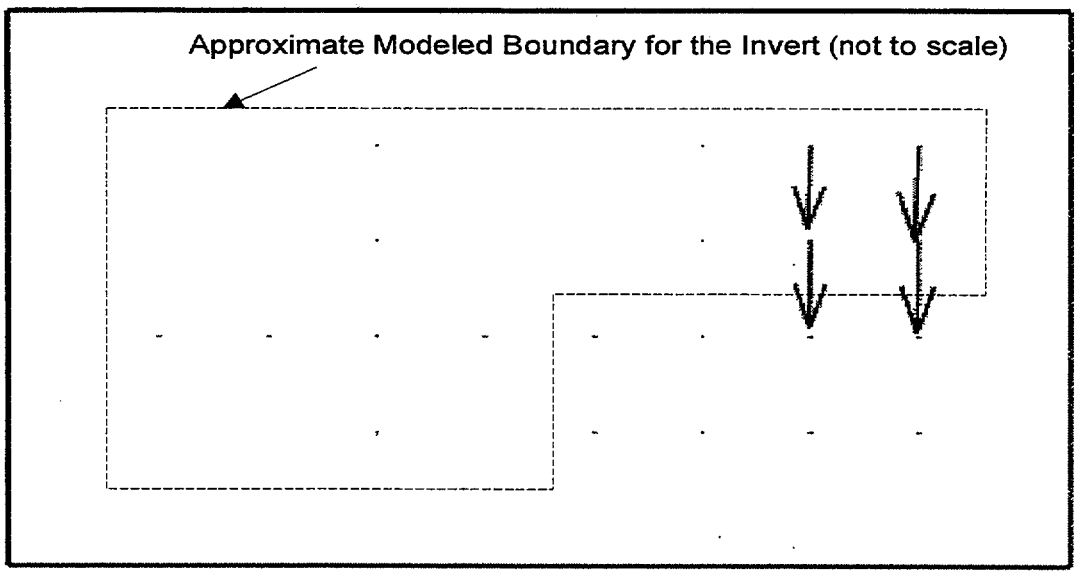

Figure 10. Fracture Pore Water Velocity Vectors in the Invert for the Case 9

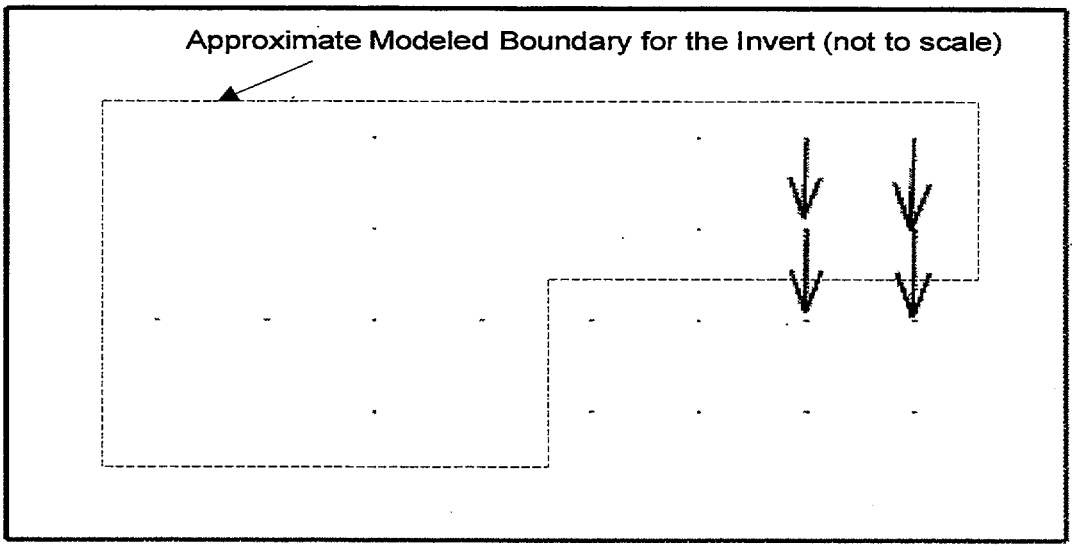

Figure 11. Matrix Pore Water Velocity Vectors in the Invert for the Case 9

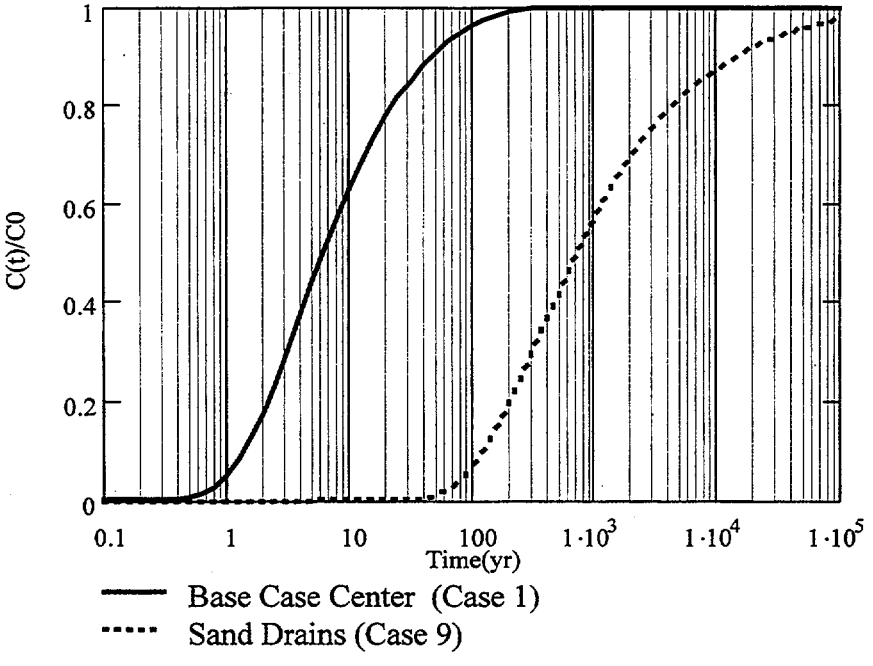

Figure 12. Effect of Sand Drains on Breakthrough for the Glacial Climate

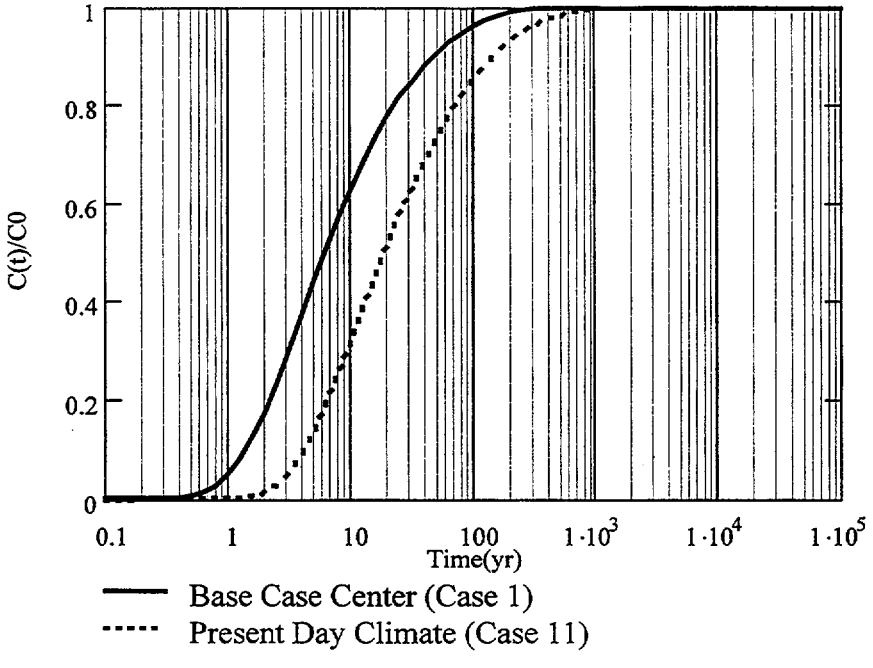

Figure 13. Comparison of the Glacial Climate to the Present Day Climate on Breakthrough

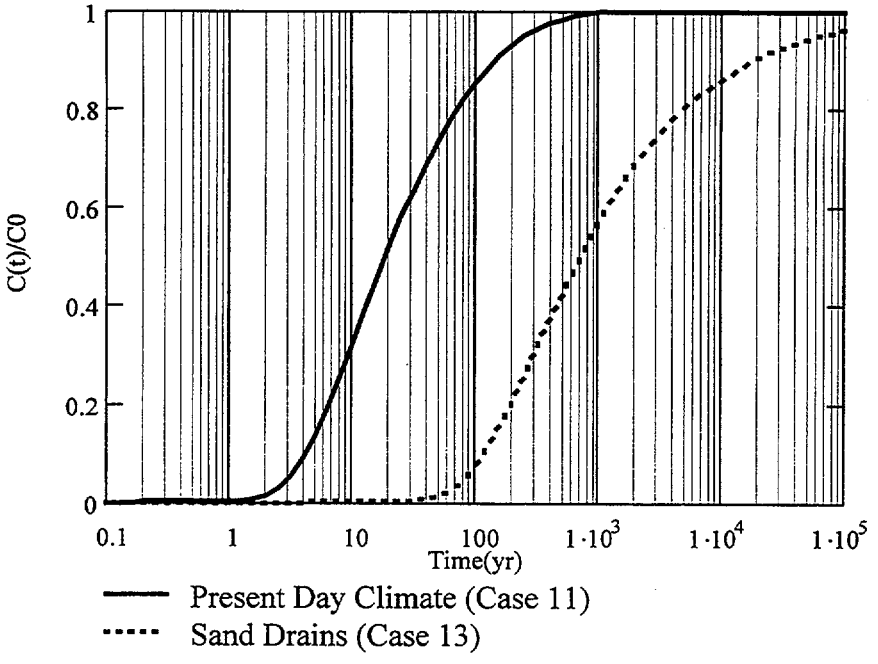

Figure 14. Effect of Sand Drains for the Present Day Climate

6.3.3 Sensitivity of Calculated Results to Variations in Physical, Hydrological, and Chemical Parameters in the EBS

This section provides a sensitivity analysis for radionuclide transport in solute or radionuclides adsorbed onto colloidal particles in the invert. This section applies the solution to the one-dimensional solute transport equation (Equation 2) and performs Monte-Carlo simulations to determine the distribution of times to breakthrough for a given distribution of input parameters listed in Table 4. Also, this section determines the sensitivity of the resulting output distribution due to each input parameter.

The retardation factor for unsaturated flow is obtained by substituting the volumetric water content for porosity and using $(1-\phi)\rho_s$ to obtain the bulk density (Jury et al. 1991, p. 227):

$$R = 1 + \frac{(1-\phi)\rho_s K_d}{\theta} \qquad \text{(Eq.13)}$$

The one-dimensional solute transport equation may be solved with the input of nine parameters listed for the base case in Table 4 for the range of parameters discussed previously. The parameters in Table 4 used in the Monte Carlo Simulation for the sensitivity analysis (Attachment III) are assumed to be uncorrelated (Section 5.13). The technical basis for this assumption is that with the exception of the volumetric moisture content, and the Darcy Flux the remaining parameters represent independent processes. For the case of these two parameters, the

Darcy Flux and the volumetric moisture content would depend directly on the percolation rate that would vary at the repository horizon. However, the volumetric moisture content would be near the residual moisture content as determined in the *Water Distribution and Removal Model Input Transmittal* (CRWMS M&O 2000d, Item 1, p.69). For purposes of scoping analysis, it is reasonable to assume that these parameters are independent.

Attachment III presents in detail the calculational method of the sensitivity analysis and the results for the relative concentration profiles as a function of time. The times to $C/C_0 = 0.01$ and 0.5, taken as first appearance and breakthrough times, respectively, are obtained from this calculation method.

The EBS Radionuclide Transport Model (Attachment III, p.1) uses Crystal Ball to perform the uncertainty/sensitivity analysis on the input parameters described in Table 4.

The simulations were run for 1,000 iterations using the data input distributions and ranges specified previously. The random seed was fixed at 1 to allow reproducibility of the results. The type of sampling was set to Latin Hypercube to increase the sampling at the tails of the distributions (although this type of sampling does not improve the efficiency when all distributions are uniform). Sensitivity analysis was turned on and correlations were turned off (Section 5.13).

Five simulations were performed. In the five simulations, the range of the partition coefficient was changed as follows: 0-1, 1-5, 5-10, 10-50, and 50-100 cm^3/g (Section 5.11) . The first set of five simulations was performed for a Darcy velocity ranging from 0 to 0.0042 m/yr and volumetric water content ranging from 0.05 to 0.07. In the second set of five simulations, range of the Darcy velocity was not changed, but the volumetric water content was increased by a factor 2, ranging from 0 to 0.14. In the final set of five simulations, the Darcy velocity was reduced by a factor of 4, ranging from 0 to 0.001 m/yr; the volumetric water content was left to range from 0.05 to 0.07. In all fifteen simulations, the range of values for all other parameters listed previously were not changed.

Table 5 below is a summary of the results. The results show that the breakthrough time for radionuclides increases with increasing sorption. Sorption represents a most sensitive parameter. An invert comprised of a sorptive material would substantially delay the release of radionuclides. Further the results show that the Darcy Flux is the most sensitive parameter while the molecular diffusion coefficient was the least sensitive parameter. Dispersivity, transport length, and volumetric moisture content were of intermediate sensitivity.

Table 5. Summary of Sensitivity/Uncertainty Analysis on One-Dimensional Solute Transport Equation

Kd Range, ml/g (Mean)	5 th Percentile of Time (y) to C/Co =		50 th Percentile Time (y) to C/Co =		Sensitivity Ranking
	0.01	0.5	0.01	0.5	
0-1 (0.5)	2	16	13	104	**J_w, Kd,** α, L, ϕ, θ, ρ_s, D_{wl}
1-5 (3)	17	166	74	590	**J_w, α_l, Kd,** L, ϕ, θ, ρ_s, D_{wl}
5-10 (7.5)	52	534	189	1487	**J_w, α_l,** L, ϕ, θ, Kd, ρ_s, D_{wl}
10-50 (30)	162	1618	730	5842	**J_w, α_l, Kd,** L, ϕ, θ, ρ_s, D_{wl}
50-100 (75)	520	5316	1883	14784	**J_w, α_l,** L, ϕ, θ, Kd, ρ_s, D_{wl}

Notes:

1. The following is a definition of the parameters listed in the sensitivity ranking, including range and mean for the simulations. All distributions were assumed to be uniform. Boldface indicates absolute value of correlation coefficient is greater than or equal to 0.2. Boldface italic indicates absolute value of correlation coefficient is greater than or equal to 0.5.
2. Nomenclature for the table

L = Transport distance (0.5-0.7 m, 0.6 m)
J_w = Darcy velocity (0-0042 m/yr, 0.0021 mm/yr)
Kd = Distribution coefficient (See column 1)
ϕ = Porosity (0.28-0.55, 0.41)
ρ_s = Grain density (2.49-2.72 g/cc, 2.61 g/cc)
θ = Volumetric water content (0.05-0.07, 0.06)
α_l = Dispersivity (0.004-0.1 m, 0.052 m)
D_{wl} = Molecular diffusion coefficient (0.035 – 0.11 m^2/yr, 0.074 m^2/yr)

6.4 MODEL VALIDATION

The EBS Radionuclide Transport Model AMR was prepared using commercial software supplemented by other standard calculations. In accordance with AP-3.10Q, Section 5.3c, the model was validated by reviewing model calibration parameters for reasonableness, or consistency. This included documentation of: parameter input, assumptions, simplifications, initial and boundary conditions; and explanation of how the software was used. The expected source of uncertainty (Input Tracking, in accordance with AP-3.15Q); and computer data files to allow independent repetition of the model simulation has been provided. The intended use of this analysis and model is to determine the sensitivity of radionuclide transport to various input transport parameters. The model is not used for assessing post-closure system performance. It is a reasonably conservative one-dimensional model that solves the advective-dispersive-diffusive transport equation. This equation is well known and widely accepted as the equation that describes radionuclide transport in porous media. Therefore, the confidence level is high for the model's intended use. The results are intended to be used in the Engineered Barrier System Degradation, Flow and Transport Process Model Report. It is not expected to be used in any other PMR or AMR.

7. CONCLUSIONS

7.1 SUMMARY

This AMR quantifies and evaluates radionuclide transport within the emplacement drift, as a result of releases from one or more breached waste packages. This AMR uses information developed in the *Water Distribution and Removal Model* (CRWMS M&O 2000d) to develop contaminant breakthrough curves. The major conclusions from this AMR are as follows:

- An analysis was performed for the glacial climate using the one dimensional advection/dispersion/diffusion equation for contaminant transport through the invert. For the parameter set used (Table 4), the results show that the breakthrough is substantial after 10 years, and is complete after 100 years. Comparable results were obtained for the present day climate. Also, the analysis shows that for areas adjacent to the centerline of the invert the breakthrough occurs more rapidly. As the distance increases from the centerline, pore water velocities in the vertical direction become larger with breakthrough occurring sooner.

- The calculated values for soil-liquid diffusion (D_{sl}) of $1.25*10^{-6}$ cm^2/sec, and hydrodynamic dispersion (D_{lh}) $9.82*10^{-7}$ are of comparable magnitude for the input parameters in Table 4. While the analysis shows that there is a reduction in flux rates within the invert due to the formation of a dry shadow below the drip shield, it also shows that for the input parameters used in this analysis (Table 4), that the porewater velocity is sufficiently high that hydrodynamic dispersion is significant.

- For the case of plugged fractures with a sand drain, not considered in the LADS EDA II repository configuration, the breakthrough time for plug flow through a length of 0.61 m is estimated to be 47,000 years for the present day climate, and 13,000 years for the glacial climate. The breakthrough times for plug flow for the case of the sand drain are three orders of magnitude higher than the base case.

- The results for radionuclide breakthrough curve using the advection/dispersion/diffusion for the case of sand drains with plugged fractures show that the breakthrough is substantially delayed (Figure 12) in comparison with the base case. Also, the analysis shows that for areas adjacent to the centerline of the invert that breakthrough is also substantially delayed.

- The *EBS Radionuclide Transport Model* uses Crystal Ball to perform the uncertainty/sensitivity analysis on the input parameters described in Table 4. Five simulations were performed. In each set of five simulations, the range of the distribution coefficients was changed as follows: 0-1, 1-5, 5-10, 10-50, and 50-100 cm^3/g. The first set of five simulations was performed for a Darcy velocity ranging from 0 to 0.0042 m/yr and volumetric water content ranging from 0.05 to 0.07 (See Attachment III). Sorption represents a most sensitive parameter. An invert comprised of a sorptive material would substantially delay the release of radionuclides. Further the results show that the Darcy Flux is the most sensitive parameter while the molecular diffusion coefficient was the least sensitive parameter. Dispersivity, transport length, and volumetric moisture content were of intermediate sensitivity.

This document may be affected by technical product input information that requires confirmation. Any changes to the document that may occur as a result of completing the confirmation activities will be reflected in subsequent revisions. The status of the input information quality may be confirmed by review of the Document Input Reference System database.

7.2 ASSESSMENT

This analysis used the results from *Water Distribution and Removal Model Input Transmittal* (CRWMS M&O 2000d, Item 1) to estimate pore water velocity, and volumetric moisture content to evaluate breakthrough through the invert used in the one dimensional advection/dispersion/diffusion equation. These methods are based on project accepted approaches for performing hydrologic and contaminant transport analysis. The results described in the *Water Distribution and Removal Model Input Transmittal* are based on unqualified technical information and unqualified software. Therefore, the use of any unqualified technical information or results from this model as input in documents supporting construction, fabrication, or procurement, or as part of a verified design to be released to another organization, is required to be identified and controlled in accordance with appropriate procedures.

7.3 TBV IMPACT

The results presented in this report are based partially on unqualified data, e.g. porosity (Section 4.1.1.2), grain density (Section 4.1.1.3), volumetric moisture content (Section 4.1.2.1), average pore water velocity (Section 4.1.2.2) and qualified data with a Verification Level 2 e.g. dry bulk density (Section 4.1.1.2). When these data are verified, an assessment of the impacts to this study as a result of any changes to the data would be required. The impact of TBVs associated with initial use assumptions is as follows:

- Section 5.9 involves the assumption of hydrodynamic dispersivity. It is expected that this TBV would have some impact on the breakthrough of long-lived radionuclides since diffusion and hydrodynamic dispersivity were found to be of comparable magnitude.

- Section 5.10 involve identifying the crushed tuff as the invert source material and using the hydrologic and geotechnical properties for this material. This TBV may have some impact on future hydrologic analyses since these properties influence the predicted saturation levels and pore water velocities in the invert.

8. REFERENCES

8.1 DOCUMENTS CITED

CRWMS M&O (Civilian Radioactive Waste Management System Management and Operating Contractor)1997. *Determination of Available Volume for Repository Siting* BCA000000-01717-0200-00007 REV 00. Las Vegas, Nevada: CRWMS M&O. ACC: MOL.19971009.0699.

CRWMS M&O 1998. *Cross Drift Geotechnical Predictive Report: Geotechnical Data Report.* BABEA0000-01717-5705-00001 REV 01. Las Vegas, Nevada: CRWMS M&O. ACC: MOL.19980922.0154.

CRWMS M&O 1999a. *Classification of the MGR Ex-Container System.* ANL-XCS-SE-000001 REV 00. Las Vegas, Nevada: CRWMS M&O. ACC: MOL.19990928.0221.

CRWMS M&O 1999b. Not Used.

CRWMS M&O 1999c. *Engineered Barrier System Process Modeling for Process Model Report - Site Recommendation (WP# 1201213EM1).* Activity Evaluation, October 11, 1999. Las Vegas, Nevada: CRWMS M&O. ACC: MOL.19991012.0118.

CRWMS M&O 1999d. *Request for Repository Subsurface Design Information to Support TSPA-SR.* Input Transmittal PA-SSR-99218.Ta. Las Vegas, Nevada: CRWMS M&O. ACC: MOL.19990901.0312

CRWMS M&O 2000a. *Development Plan for EBS Radionuclide Transport Model.* TDP-EBS-MD-000009 REV 02. Las Vegas, Nevada: CRWMS M&O. URN-240. Submitted to RPC.

CRWMS M&O 2000b. *Invert Diffusion Properties Model.* ANL-EBS-MD-000031 REV 00. Las Vegas, Nevada: CRWMS M&O. ACC: MOL.20000203.0694.

CRWMS M&O 2000c. *Waste Package Degradation Process Model Report.* TDR-WIS-MD-000002 REV 00. Las Vegas, Nevada: CRWMS M&O. ACC: MOL.20000328.0322.

CRWMS M&O 2000d. *Water Distribution and Removal Model.* Input Transmittal 00083.T. Las Vegas, Nevada: CRWMS M&O. ACC:MOL.20000310.0060.

CRWMS M&O 2000e. *Water Diversion Model.* ANL-EBS-MD-000028 REV 00. Las Vegas, Nevada: CRWMS M&O. ACC: MOL.20000107.0329.

de Marsily, G. 1986. *Quantitative Hydrogeology: Groundwater Hydrology for Engineers.* San Diego, California: Academic Press. TIC: 208450.

Fang, H-Y., ed. 1991. *Foundation Engineering Handbook.* 2nd Edition. Boston, Massachusetts: Kluwer Academic Publishers. TIC: 245696.

Fetter, C.W. 1993. *Contaminant Hydrogeology.* New York, New York: Macmillan Publishing. TIC: 240691.

Freeze, R.A. and Cherry, J.A. 1979. *Groundwater.* Englewood Cliffs, New Jersey: Prentice-Hall. TIC: 217571.

Hahn, G.J. and Shapiro, S.S. 1968. *Statistical Models in Engineering.* 1st Edition. New York, New York. John Wiley & Sons. Library Tracking No.: L1463.

Hardin, E.L. 1998. *Near-Field/Altered-Zone Models Report.* UCRL-ID-129179. Livermore, California: Lawrence Livermore National Laboratory. ACC: MOL.19980630.0560.

Jury, W.A.; Gardner, W.R.; and Gardner, W.H. 1991. *Soil Physics.* 5th Edition. New York, New York: John Wiley & Sons. TIC: 241000.

Mathsoft 1998. *Mathcad 8, User's Guide.* Cambridge, Massachusetts: MathSoft. TIC: 242289.

Mills, R. 1973. *"Self-Diffusion in Normal and Heavy Water in the Range 1-45degrees."* The Journal of Physical Chemistry, 77 (5), 685-688. Washington, D.C.: American Chemical Society. TIC: 246404.

Philip, J.R.; Knight, J.H.; and Waechter, R.T. 1989. *"Unsaturated Seepage and Subterranean Holes: Conspectus, and Exclusion Problem for Circular Cylindrical Cavities."* Water Resources Research, 25 (1), 16-28. Washington, D.C.: American Geophysical Union. TIC: 239117.

Wilkins, D.R. and Heath, C.A. 1999. *"Direction to Transition to Enhanced Design Alternative II."* Letter from Dr. D.R. Wilkins (CRWMS M&O) and Dr. C.A. Heath (CRWMS M&O) to Distribution, June 15, 1999, LV.NS.JLY.06/99-026, with enclosures, *"Strategy for Baselining EDA II Requirements"* and *"Guidelines for Implementation of EDA II."* ACC: MOL.19990622.0126; MOL.19990622.0127; MOL.19990622.0128.

8.2 CODES, STANDARDS, REGULATIONS, AND PROCEDURES

AP-2.13Q, Rev. 0, ICN 1. *Technical Product Development Planning.* Washington, D.C.: U.S. Department of Energy, Office of Civilian Waste Management. ACC: MOL.19991115.0230.

AP-3.10Q, Rev. 2. *Analyses and Models.* Washington, D.C.: U.S. Department of Energy, Office of Civilian Radioactive Waste Management. ACC: MOL.20000217.0246.

AP-3.15Q, Rev. 1, ICN 1. *Managing Technical Product Inputs.* Washington, D.C.: U.S. Department of Energy, Office of Civilian Radioactive Waste Management. ACC: MOL.20000218.0069.

AP-SI.1Q, Rev. 2, ICN 4. *Software Management*. Washington, D.C.: U.S. Department of Energy, Office of Civilian Radioactive Waste Management. ACC: MOL.20000223.0508.

AP-SIII.3Q, Revision 0, ICN 2. *Submittal and Incorporation of Data to the Technical Data Management System*. Washington, D.C.: U.S. Department of Energy, Office of Civilian Radioactive Waste Management. ACC: MOL.19991214.0632

DOE (U.S. Department of Energy) 2000. *Quality Assurance Requirements and Description*. DOE/RW-0333P, Rev. 9. Washington, D.C.: U.S. Department of Energy, Office of Civilian Radioactive Waste Management. ACC: MOL.19991028.0012.

QAP-2-0, Revision 5. *Conduct of Activities*. Las Vegas, Nevada: CRWMS M&O. ACC: MOL.19980826.0209.

QAP-2-3, Revision 10. *Classification of Permanent Items*. Las Vegas, Nevada: CRWMS M&O. ACC: MOL.19990316.0006.

8.3 SOURCE DATA, LISTED BY DATA TRACKING NUMBER

GS980808312242.015. Water Retention And Unsaturated Hydraulic Conductivity Measurements For Various Size Fractions Of Crushed, Sieved, Welded Tuff Samples Measured Using A Centrifuge. Submittal Date: 08/21/1998.

SN9908T0872799.004. Tabulated In-Drift Geometric and Thermal Properties Used in Drift-Scale Models for TSPA-SR (Total System Performance Assessment - Site Recommendation). Submitted date: 08/30/1999.

SNL02030193001.027. Summary of Bulk Property Measurements Including Saturated Bulk Density for NRG-2, NRG-2A, NRG-2B, NRG-3, NRG-4, NRG-5, NRG-6, NRG-7/7A, SD-9 and SD-12. Submittal Date: 08/14/1996.

MO0003SEPRWDRM.001.Results from Water Distribution and Removal Model. Submittal Date: 03/23/2000.

ATTACHMENT I

DE MARSILY's ONE DIMENSIONAL TRANSPORT EQUATION USING EXCEL SPREADSHEET

ATTACHMENT I

I.1 SPREADSHEET IMPLEMENTATION

A Microsoft Excel 97 spreadsheet titled *One-dimensional-flow_V.1.xls* contains the Crystal Ball routine. Table I-1 presents part of this spreadsheet. This spreadsheet in its entirety is contained on a floppy that is included with this attachment. It is used to implement Equation 2 (Section 6.2.2) to calculate the relative concentration profiles as a function of time. The nine input parameters (Section 6.2.3, Table 4) may be entered manually, or may be changed automatically by the uncertainty analysis module.

Table I-1. Spreadsheet for Averaged Concentration versus Time

Inputs		Input Sources (Section number when applicable)		
(t) maximum time, yr	1.00E+07	Upper limit for time on graphic plot		
(L) path length distance, m *	0.61	Section 4.1.1.1		
(Jw) Darcy flux, m/yr	0.0022	Section 5.1.4	mm/yr	2.20E+00
(Kd) linear reversible partition coefficient, mL/g *	0	Section 5.11		
(ϕ) porosity *	0.545	Section 4.1.1.2		
(λ) Jury dispersivity, m	0.1	Section 5.8	cm	1.00E+01
(ps) grain density, g/cc	2.53	Section 4.1.1.3		
(θ) volumetric moisture content *	0.071	Section 4.1.2.2		
(α_L) de Marsily dispersivity, λ/θ , m	1.41	Calc - dispersivity as defined in de Marsily, 1986		
(Dwl) molecular diffusion coefficient, m^2/yr	7.3E-02	Section 5.5	cm^2/sec	2.30E-05
(τ) tortuosity (θ^2/ϕ^0.7)	7.71E-03	Calc		
(Dsl) solute diffusion coefficient (τ*Dwl), m^2/yr	5.59E-04	Calc	cm^2/sec	1.77E-07
(Dlh) longitudinal hydrodynamic dispersion (α_L*Jw),	3.10E-03	Calc	cm^2/sec	9.83E-07
(De) diffusion-dispersion coefficient (θ*Dsl + Dlh), m^2/yr	3.14E-03	Calc	cm^2/sec	9.95E-07
(R) retardation (1 + (1-ϕ)*ps*Kd/θ)	1.00E+00	Calc		
A1 = (Jw)/(θ*R*L)	5.08E-02	Calc		
B1 = 2*sqrt(De/(θ*R))/L	6.89E-01	Calc		
C1 = Jw*L/De	4.28E-01	Calc		

* denotes Crystal Ball Assumptions (See Attachment III)

c(x,t) relative concentration (C/Co) = 0.5*(erfc((1-A1*t)/(B1*sqrt(t))) + exp(C1)*erfc((1+A1*t)/(B1*sqrt(t))))

Reference: de Marsily (1986, pp .268 and 276)

Factors for interpolation (Using Excel lookup function on Table I-2)

Target Concentration	Time 1	C/Co	Time 2	C/Co
0.01	5.99E-01	9.9232E-03	6.31E-01	1.2101E-02
0.5	6.17E+00	4.9832E-01	6.49E+00	5.1278E-01

Interpolated values (using Excel forecast function between Time 1 and Time 2)

Time to C/Co=0.01	6.0E-01	years
Time to C/Co=0.5	6.2E+00	years

Crystal Ball Forecast Cells
See Attachment III

Due to limitations in the way Excel calculates the complementary error function (erfc), two error-checking columns were added to the spreadsheet (one for each instance the complementary error function occurs in Equation 2). The purpose of these columns is to adjust any errors returned by the complementary error function when the argument exceeds the allowable range in Excel. The values are set to zero when the argument is less than zero or two when the argument exceeds zero.

To report the results, a table of times vs. relative concentration (C/C_0) is laid out for 400 logarithmically spaced time intervals from 0.01 to 10 million years (See the *Microsoft Excel 97* spreadsheet titled *One-dimensional-flow_V.1.xls* that contains the Crystal Ball routine). The times to $C/C_0 = 0.01$ and 0.5, taken as first appearance and breakthrough times, respectively, are obtained by using Excel's vertical lookup function coupled with linear interpolation using Excel's "Forecast"function.

The vertical lookup function captures the time at which the relative concentration is closest to, but less than, the target relative concentration (either 0.01 or 0.5). The next time step will then produce a relative concentration that is greater than the selected target. The forecast function uses the target relative concentration, in conjunction with the two time-concentration pairs surrounding the target, to estimate the time at which the target concentration occurs. This method is more robust than using Excel's "Goal Seek" function.

The same input parameters values used in the example calculation (from Table 4) were entered on in the Excel spreadsheet. The vertical lookup function produced the results reported in Table I-2.

Table I-2. Results of Excel Vertical Lookup Function for Target Relative Concentrations set to 0.01 and 0.5

Target Concentration	Time 1 (yr)	C/C_o at Time 1	Time 2 (yr)	C/C_o at Time 2
0.01	0.599	0.00992	0.631	0.0121
0.5	6.17	0.498	6.49	0.513

The Excel forecast function returned a result of 0.60 and 6.2 years for a target set to 0.01 and 0.5, respectively. The breakthrough time of 6.2 years ($C/C_o = 0.5$) matches the results obtained in the example hand calculation presented in Attachment II.

The Excel spreadsheet also displays the data as a graph. The plot of relative concentration as a function of time for the previous example is given in Figure I-1. For comparison, another plot is shown in Figure I-2 for a distribution coefficient of 1 cm^3/g. Note the shift of the second curve to the right, indicating the retardation of the solute.

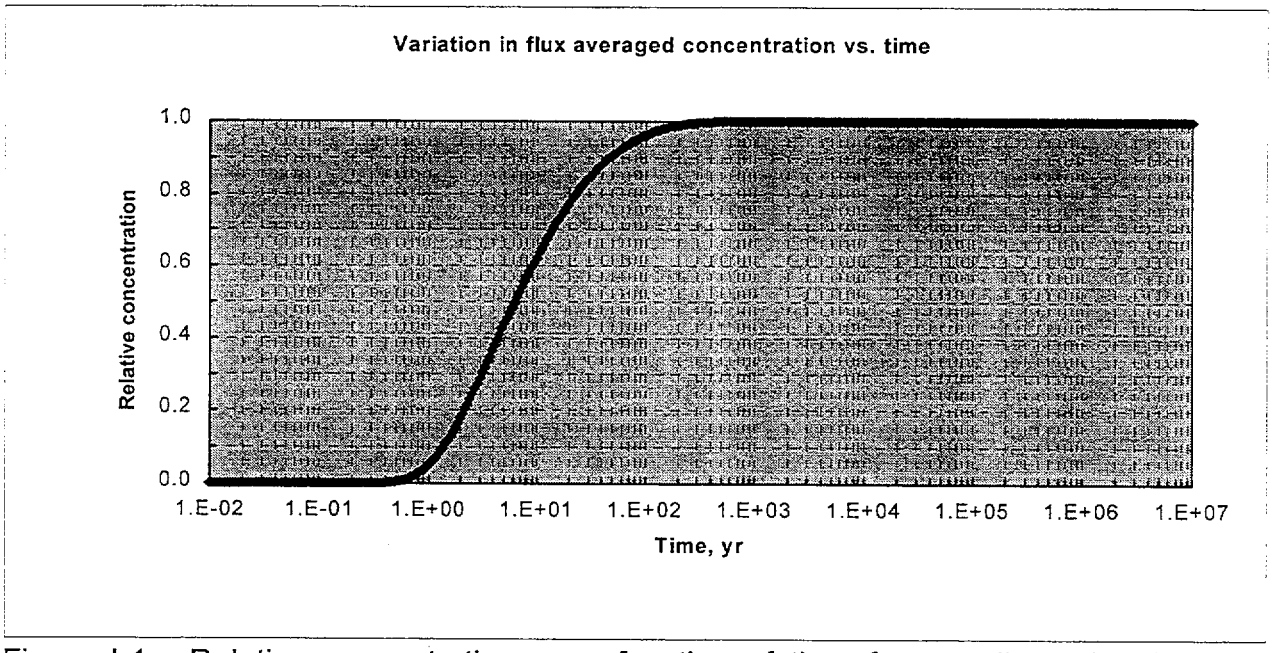

Figure I-1. Relative concentration as a function of time for one-dimensional solute transport equation using parameters in Table 4.

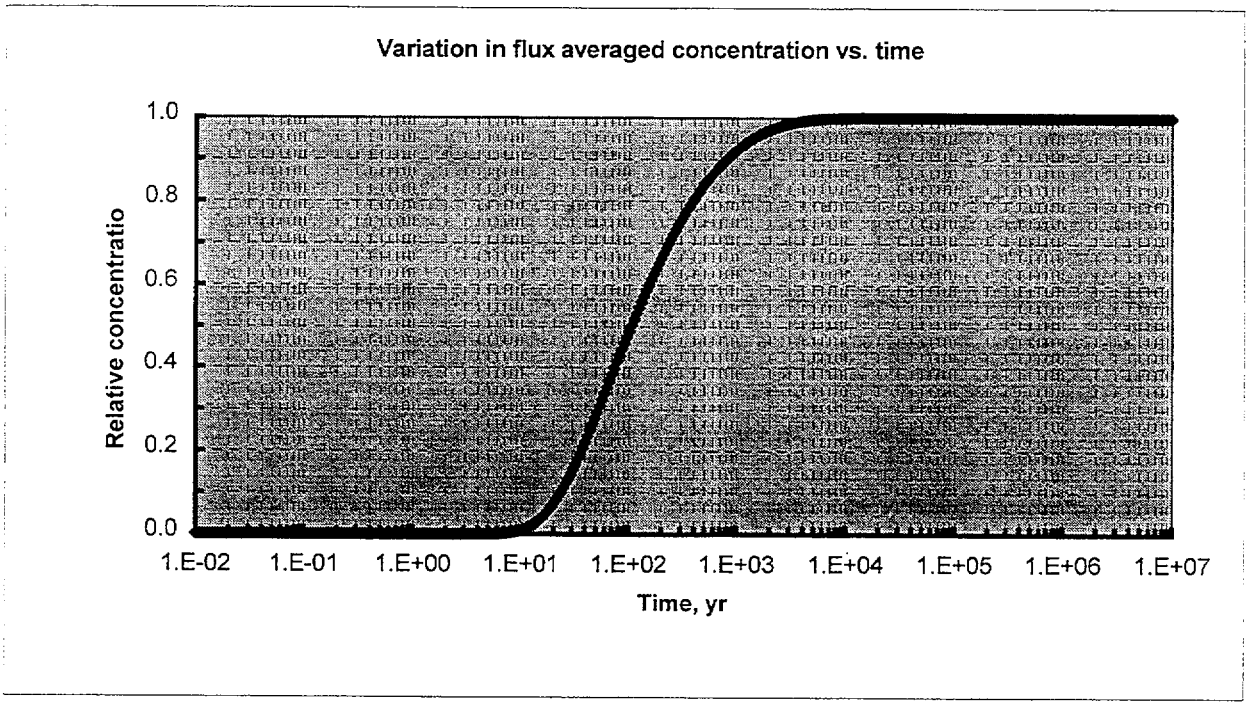

Figure I-2. Relative concentration as a function of time for one-dimensional solute transport equation using parameters in Table 4, except for the partition coefficient ($1 cm^3/g$).

Intentionally Left Blank

ATTACHMENT II

VERIFICATION OF DE MARSILY'S ONE-DIMENSIONAL CONTAMINANT TRANSPORT EQUATION BY HAND CALCULATION

ATTACHMENT II

II.1 CALCULATION METHOD

The one-dimensional advection-dispersion equation for saturated porous media is (de Marsily 1986, p. 268):

$$C(x,t) = \frac{C_o}{2}\left[\operatorname{erfc}\left(\frac{L-(J_w/\phi R)t}{2\sqrt{Dt/\phi R}}\right) + \exp\left(\frac{J_w L}{D}\right)\operatorname{erfc}\left(\frac{L+(J_w/\phi R)t}{2\sqrt{Dt/\phi R}}\right)\right] \qquad \text{(Eq.II-1.)}$$

where

C(x, t) = solute concentration at location x and time t
C_o = solute concentration at x = 0 and t = 0
erfc = complementary error function
L = distance, m
t = time, yr
J_w= darcy flux, m/yr
ϕ= porosity, dimensionless
D = diffusion-dispersion coefficient, m^2/yr
R = retardation factor, dimensionless

To function effectively as a diffusion barrier, the invert material must be largely unsaturated, with low volumetric flux. For unsaturated flow , the volumetric moisture content will be less than the porosity, and the transport equation becomes:

$$C(x,t) = \frac{C_o}{2}\left[\operatorname{erfc}\left(\frac{L-(J_w/\theta R)t}{2\sqrt{Dt/\theta R}}\right) + \exp\left(\frac{J_w L}{D}\right)\operatorname{erfc}\left(\frac{L+(J_w/\theta R)t}{2\sqrt{Dt/\theta R}}\right)\right] \qquad \text{(Eq.II-2.)}$$

where

θ = volumetric water content, dimensionless

The retardation factor, R, for unsaturated flow is derived from Jury et al. (1991, p. 227) by substuting the volumetric water content for porosity (to account for an unsaturated medium) and using $(1-\phi)\rho_s$ to obtain the bulk density:

$$R = 1 + \frac{(1-\phi)\rho_s\, Kd}{\theta} \qquad \text{(Eq.II-3.)}$$

where

ρ_s = grain density, g/cm^3 or g/mL
Kd = linear reversible partition coefficient, cm^3/g or mL/g

The diffusion-dispersion coefficient for unsaturated flow is obtained by substuting the volumetric water content for porosity (de Marsily 1986, p. 238):

$$D = \theta D_{sl} + D_{lh} \qquad \text{(Eq. II-4.)}$$

where

D_{sl} = solute diffusion coefficient, m^2/yr
D_{lh} = longitudinal hydrodynamic dispersion, m^2/yr

The solute diffusion coefficient is from the *Invert Diffusion Properties Model* (CRWMS M&O 2000b, p. 20):

$$D_{sl} = \tau D_{wl} \qquad \text{(Eq.II-5.)}$$

where D_{wl} is the molecular diffusion coefficient, m^2/yr, and τ is the tortuosity given by:

$$\tau = \frac{\theta^2}{\phi^{0.7}} \qquad \text{(Eq.II-6.)}$$

Note: The equation shown here is cast in terms of the volumetric water content and the porosity rather than saturation and porosity as expressed in the above reference.

The longitudinal hydrodynamic dispersion is (de Marsily 1986, p. 238):

$$D_{lh} = \alpha_l J_w \qquad \text{(Eq.II-7.)}$$

where

α_l = longitudinal dispersivity, m

The equation derived in de Marsily (1986, p. 238) for longitudinal hydrodynamic dispersion (Equation II-7 in this Attachment) uses a form of dispersivity that is the dispersivity as defined by Jury et al. (1991, p. 222) divided by the volumetric water content. Therefore, the range of input values will be a function of both Jury dispersivity and volumetric water content.

Equations II-2 through II-7 can be used to determine the time to breakthrough for unsaturated transport, defined as the time it takes for the concentration at the point of output to reach one half of the concentration at the point of input. Sample input parameters are provided in Table 4.

The retardation factor, R, is given by Equation II-3 and yields a value of 1 using the parameters in Table 4:

$$R = 1 + \frac{(1-0.545)2.53 \cdot 0}{0.071} = 1 + 0 = 1$$

The tortuosity, τ, is given by Equation II-6 and yields a value of 0.00772:

$$\tau = \frac{0.071^2}{0.545^{0.7}} = \frac{0.0504}{0.653} = 0.00772$$

Entering this value of τ and the molecular diffusion coefficient of 0.073 m^2/yr into Equation II-5 yields an solute diffusion coefficient of 0.0006 m^2/yr:

$D_{sl} = 0.00772 \times 0.073 = 0.0006$

The longitudinal hydrodynamic dispersion is calculated with Equation II-7 (dividing the Jury dispersivity by the volumetric water content to obtain the de Marsily dispersivity), yielding a value of 0.0031 m^2/yr:

$D_{lh} = (0.1/0.071) \times 0.0022 = 1.4 \times 0.0022 = 0.0031$

The effective diffusion-dispersion coefficient is given by Equation II-4 and yields a value of 0.00314 m^2/yr:

$D_e = (0.071 \times 0.0006) + 0.0031 = 0.000040 + 0.0031 = 0.00314$

The solution for Equation II-2 is sought for the time t at which $C/C_o = 0.5$.

Therefore, $\left[\text{erfc}\left(\frac{L-(J_w/\theta R)t}{2\sqrt{Dt/\theta R}}\right) + \exp\left(\frac{J_w L}{D}\right)\text{erfc}\left(\frac{L+(J_w/\theta R)t}{2\sqrt{Dt/\theta R}}\right)\right]$ must be set to 1.

In the above expression:

$J_w/\theta R = 0.0022/(0.071 \times 1) = 0.0310$

$$2\sqrt{Dt/\theta R} = \sqrt{4D/\theta R} \times \sqrt{t} = \sqrt{\frac{4 \times 0.00314}{0.071 \times 1}} \times \sqrt{t} = \sqrt{\frac{0.0126}{0.071}} \times \sqrt{t} = \sqrt{0.177} \times \sqrt{t} = 0.421\sqrt{t}$$

$$\exp\left(\frac{J_w L}{D}\right) = \exp\left(\frac{0.0022 \times 0.61}{0.00314}\right) = \exp\left(\frac{0.00134}{0.00314}\right) = \exp(0.427) = 1.53$$

Entering the these values, and a path length of 0.61 m (Section 4.1.1.1), yields the following expression:

$$\left[\operatorname{erfc}\left(\frac{0.61-0.0310t}{0.421\sqrt{t}}\right)+1.53\operatorname{erfc}\left(\frac{0.61+0.0310t}{0.421\sqrt{t}}\right)\right]=1$$

By trial and error, a value of t = 6.20 yr is found that will solve the above expression:

$$\left(\frac{0.61-(0.0310\times 6.20)}{0.421\sqrt{6.20}}\right)=\left(\frac{0.61-0.192}{0.421\times 2.49}\right)=\frac{0.418}{1.05}=0.398$$

$$\left(\frac{0.61+(0.0310\times 6.20)}{0.421\sqrt{6.20}}\right)=\left(\frac{0.61+0.192}{0.421\times 2.49}\right)=\frac{0.802}{1.05}=0.764$$

$$\operatorname{erfc}(0.398)+1.53\operatorname{erfc}(0.764)=0.574+(1.53\times 0.280)=0.574+0.428=1.00$$

This value for time of 6.20 yr matches the value calculated by the EXCEL spreadsheet (Attachment I) for the same set of parameter values.

ATTACHMENT III

MONTE CARLO ANALYSIS

ATTACHMENT III

III.1 UNCERTAINTY AND SENSITIVITY ANALYSIS

Crystal Ball, Version 4.0e, is an *Excel* spreadsheet application used to perform the uncertainty/sensitivity analysis on the input parameters described in the Data Input section. The portions of *Crystal Ball* used in this analysis, (namely, the multiplication and division of multiple uniform distributions, and resulting statistics of output distributions) have been validated per the software management controls for software routines in AP-SI.1Q, *Software Management.* Results of this validation are presented in Attachment V.

Crystal Ball allows the user to define a number of spreadsheet cells as "input" or "assumption" cells and others as "forecast" cells. Forecast cells typically contain functions that depend on values contained in the assumption cells. Assumption cells are assigned a distribution and associated parameters, which depend on the selected distribution type. For example, an input that is assigned a uniform distribution requires a minimum and maximum value for that distribution. In addition, another cell may be correlated with another input cell by specifying the degree of correlation from -1 to 1.

The simulation is controlled by a set of instructions. The most important ones affecting the results of the calculation include a fixed or random initial random number seed, the number of iterations to be executed, the type of sampling (Monte Carlo or Latin Hypercube), sensitivity on/off, and correlation on/off. All except the first one affect the amount of time required to run the simulation.

The simulations were run for 1,000 iterations using the data input distributions and ranges specified in Table 4 (Section 6.2.3). The random seed was fixed at 1 to allow reproducibility of the results. The type of sampling was set to Latin Hypercube to increase the sampling at the tails of the distributions (although this type of sampling does not improve the efficiency when all distributions are uniform). Sensitivity analyses was turned on and correlations were turned off (Section 5.13).

Five simulations were performed in the file *One-dimensional-flow_V.1.xls.* In each simulation, the range of the distribution coefficient was changed as follows: 0-1, 1-5, 5-10, 10-50, and 50-100 cm^3/g. The range of values for all other parameters is listed in the Input Data section, and uniform distributions were assumed for all parameters. Each simulation is detailed in the files described in Table III-1. The results of the sensitivity analyses are summerized in Table 6 (Section 6.3.3). The test of verification of the proper multiplication and division uniformly distributed variables is presented in Attachment V.

III.2 COMPUTER FILES

Table III-1 provides a list of computer files for the EBS Radionuclide Transport Model. The files are contained on the floppy included with this attachment.

Table III-1. List of Computer Files

File Name	Directory	Brief Description
REPORT1.xls	Sources Data	**For a Kd range of 0-1 cm^3/g:** Sensitivity chart; Forecasted Time to Reach a Concentration of C/C_o = 0.1; Forecasted Time to Reach a Concentration of C/C_o = 0.5; Input Parameter Ranges
REPORT2.xls		**For a Kd range of 1-5 cm^3/g :** Sensitivity chart; Forecasted Time to Reach a Concentration of C/C_o = 0.1; Forecasted Time to Reach a Concentration of C/C_o = 0.5; Input Parameter Ranges
REPORT3.xls		**For a Kd range of 5-10 cm^3/g:** Sensitivity chart; Forecasted Time to Reach a Concentration of C/C_o = 0.1; Forecasted Time to Reach a Concentration of C/C_o = 0.5; Input Parameter Ranges
REPORT4.xls		**For a Kd range of 10-50 cm^3/g:** Sensitivity chart; Forecasted Time to Reach a Concentration of C/C_o = 0.1; Forecasted Time to Reach a Concentration of C/C_o = 0.5; Input Parameter Ranges
REPORT5.xls		**For a Kd range of 50-100 cm^3/g:** Sensitivity chart; Forecasted Time to Reach a Concentration of C/C_o = 0.1; Forecasted Time to Reach a Concentration of C/C_o = 0.5; Input Parameter Ranges

ATTACHMENT IV

SENSITIVITY OF RESULTS TO THERMAL HYDROLOGICAL CHEMICAL (THC) PROCESSES

ATTACHMENT IV

IV.1 PURPOSE

This attachment presents an estimate of the contaminant transport for crushed tuff for focussed and unfocussed flow, and with and without the plugging of fractures below the invert. Two different climates are considered in the analysis. The effects of sand drains are also included in this analysis. This attachment provides verification of the functions described in Equations 2, 2a and 2b that are presented below. The results are compared with Fetter's results (See Figure IV-1) and the hand calculation presented on p.IV-6.

IV.2 METHOD

The simplest chemical transport processes in the invert are those that involve nonvolatile dissolved solutes that neither chemically react nor physically adsorb to the invert solids. The one dimensional advection-dispersion-diffusion relation for contaminant transport or breakthrough for those solutes whose vapor phase is negligible (Section 5.7) and nonreactive is analyzed for by solving Equation (1):

$$\frac{d}{dt}C_l = D\cdot\frac{d^2}{dz^2}C_l - V\cdot\frac{d}{dz}C_l$$

At t = 0, water is instantaneously introduced in the invert material and continues at a constant flux rate J_W in the vertical direction. The radionuclides are introduced to the invert material at an initial concentration C_0 at a continuous rate.

A solution to the above relation is presented by Freeze and Cherry (1979), page 391 for nonretarded transport in one dimension with initial concentration C_0 at a continuous rate in which the vapor phase transport is negligible(Sections 5.X to 5.X)) is given by Equation (2):

$$\frac{C_l}{C_o} = \frac{1}{2}\cdot\left(\operatorname{erfc}\left(\frac{L - V\cdot t}{2\cdot\sqrt{D\cdot t}}\right) + \exp\left(\frac{V\cdot L}{D}\right)\cdot\operatorname{erfc}\left(\frac{L + V\cdot t}{2\cdot\sqrt{D\cdot t}}\right)\right)$$

To evaluate Equation (2), we define the functions in MathCad 8 Professional with assignment statements. The assignment statement uses the :=.
The error function (Equation 2a) is given by (Freeze and Cherry, 1979, page 539)

$$\operatorname{erf}(\beta) = \frac{2}{\pi}\cdot\int_0^{\beta} e^{-\varepsilon^2}\,d\varepsilon$$

Define the complimentary error function (Equation 2b) for the closed form solution for breakthrough analysis. The function is used in the closed form solution for the breakthrough analysis.

$$\operatorname{erfc}(\beta) := 1 - \operatorname{erf}(\beta)$$

Define the initial concentration and concentration function for analysis. From Equation (2)

$C_o := 1$

$$C(V,t,L,R,D) := \frac{C_o}{2}\cdot\operatorname{erfc}\left[\frac{1}{2}\cdot\frac{\left(L-\frac{V}{R}\cdot t\right)}{\sqrt{\frac{D}{R}}\cdot\sqrt{t}}\right] + \frac{C_o}{2}\cdot\exp\left(\frac{V}{1}\cdot\frac{L}{D}\right)\cdot\operatorname{erfc}\left[\frac{1}{2}\cdot\frac{\left(L+\frac{V}{R}\cdot t\right)}{\sqrt{\frac{D}{R}}\cdot\sqrt{t}}\right]$$

As a test case, verify the function against the dimensionless curves shown by Fetter (1993, p.60). The Peclet Number for the solution is defined as the ratio (V*L/D) (Fetter 1993, p.58). Consider a range of Peclet Numbers from 1,10 and 100 as shown in Fetter (1993, p.60, Figure 2.9). Since the plot uses dimensionless parameters, we can define the length as of 1.0 and the diffusion-dispersion coefficient as 1.0. We then use dimensionless parameter definitions (Fetter 1993, p.58) to calculate the velocity for a given Peclet Number:

$P_e := 100$

$L := 1.0$

$D := 1.0$

From Fetter, 1993, p. 58, the velocity is given by:

$$V := \frac{P_e \cdot D}{L}$$

$V = 100$

$R := 1.0$

$t_R := 0.001, 0.01 .. 2.0$

Note that the Peclet Numbers equals (V*L/D), and the Dimensionless Time t_R equals (v*t/L).

The results presented below can be compared to the results shown in Fetter (1993, p.60, Figure 2.9). The results are compared by selecting a t_R and evaluating C to see if it matches the results in Figure 2.9.

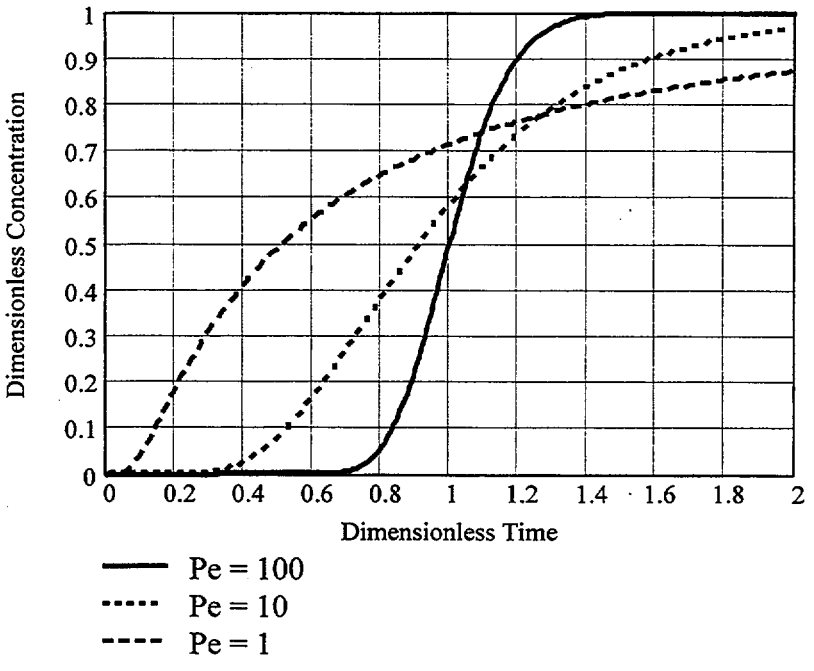

Figure IV-1 Dimensionless Type Curves for the Continuous Injection of a Tracer

Evaluate the user defined function (Equation (2)) by hand calculation at 6.2 years. Inputs are obtained from Table 4 in Section 6.2.3 which is based upon inputs (Sections 4.1).

$L := 4 \cdot 0.152 \cdot m$

$L = 0.608\,m$

$V := 31 \cdot \frac{mm}{yr}$

$\phi := 0.545$

$\theta := 0.071$

Input the dispersivity (Section 5.9)

$\lambda := 10 \cdot cm$

Input the water diffusivity (Section 5.6). Convert units to m^2/yr.

$$D_{wl} := 2.30 \cdot 10^{-5} \cdot \frac{cm^2}{sec}$$

$$D_{wl} = 0.073 \quad \frac{m^2}{yr}$$

Calculate the tortuosity (Equation (8))

$$Tr = \frac{\theta^2}{\phi^{0.7}}$$

$$T = 7.70973 \times 10^{-3}$$

Calculate the hydrodynamic dispersion (Equation (5).

$D_{lh} := \lambda \cdot V$

$$D_{lh} = 3.1 \times 10^{-3} \frac{m^2}{yr}$$

$$D_{lh} = 9.82 \times 10^{-7} \frac{cm^2}{sec}$$

Calculate the solute diffusion (Equation (8).

$D_{sl} := \tau \cdot D_{wl}$

$$D_{sl} = 5.57 \times 10^{-4} \frac{m^2}{yr}$$

$$D_{sl} = 1.77 \times 10^{-7} \frac{cm^2}{sec}$$

Calculate the diffusion coefficient(Equations (3),(5),(6) and (12)).

$$D_e := \frac{\theta^3}{\phi^{0.7}} \cdot D_{wl} + \lambda \cdot V$$

$$D_e = 3.13956 \times 10^{-3} \frac{m^2}{yr}$$

Note that D equals the De divided by the volumetric moisture content (Jury et al. 1991, p. 223)

$$D := \frac{D_e}{\theta}$$

$$D = 0.04422 \frac{m^2}{yr}$$

For purposes of verification, use the following definitions. Consider the time at 6.2 years that corresponds with an approximate breakthrough of 0.5

$$\frac{C_o}{2} \cdot \operatorname{erfc}\left[\frac{1}{2} \cdot \frac{(L - V \cdot t)}{\sqrt{D} \cdot \sqrt{t}}\right] + \frac{1}{2} \cdot \exp\left(\frac{V}{1} \cdot \frac{L}{D}\right) \cdot \operatorname{erfc}\left[\frac{1}{2} \cdot \frac{(L + V \cdot t)}{\sqrt{D} \cdot \sqrt{t}}\right]$$

Substituting in the values for the parameters presented above:

$t := 6.2 \cdot yr$

$$\frac{1.0}{2} \cdot \operatorname{erfc}\left[\frac{1}{2} \cdot \frac{(0.608 - 0.031 \cdot 6.2)}{\sqrt{0.04422} \cdot \sqrt{6.2}}\right] + \frac{1}{2} \cdot \exp\left(\frac{0.031}{1} \cdot \frac{0.608}{0.04422}\right) \cdot \operatorname{erfc}\left[\frac{1}{2} \cdot \frac{(0.608 + 0.031 \cdot 6.2)}{\sqrt{0.04422} \cdot \sqrt{6.2}}\right]$$

Simplifying the expression:

$$\frac{1.0}{2} \cdot \operatorname{erfc}(.397057) + \frac{1}{2} \cdot \exp(.426232) \cdot \operatorname{erfc}(.764123)$$

Evaluate the complementary error functions. From Freeze and Cherry 1979, p.539. Use linear interpolation.

$$\text{Table} := \begin{pmatrix} 0.35 & 0.620618 \\ 0.40 & 0.571608 \end{pmatrix}$$

$\text{linterp}(\text{Table}^{\langle 0 \rangle}, \text{Table}^{\langle 1 \rangle}, 0.397057) = 0.57449$

$\operatorname{erfc}(0.397057) = 0.57444$

$$\text{Table} := \begin{pmatrix} 0.75 & 0.288844 \\ 0.80 & 0.257899 \end{pmatrix}$$

$\text{linterp}(\text{Table}^{\langle 0 \rangle}, \text{Table}^{\langle 1 \rangle}, 0.764123) = 0.2801$

Substituting the complementary error function evaluations.

$\operatorname{erfc}(0.764123) = 0.27986$

$\frac{1.0}{2} \cdot 0.57449 + \frac{1}{2} \cdot \exp(.426232) \cdot 0.2801 = 0.50173$

Output the results from the function definition.

$C(V,t,L,R,D) = 0.50152$

The answer from the user defined function based upon Equation (2) agrees with hand calculation presented above to three significant figures.

IV.3 ANALYSIS OF THE CRUSHED TUFF INVERT

The following calculations present an analysis of a diffusive barrier. This section presents an analysis of a diffusive barrier 0.61 meters thick for the cases and two columns analyzed Item 1 of the *Water Distribution and Removal Model Input Transmittal* (Sections 4.1.2.1 to 4.1.2.2). Note that each row corresponds to different cases, and each column to the two columns of grid blocks.

$$\begin{pmatrix} 1 \\ 2 \\ 3 \\ 4 \\ 9 \\ 10 \\ 11 \\ 12 \\ 13 \end{pmatrix} \quad V := \begin{pmatrix} 31 & 74 \\ 33 & 77 \\ 33 & 77 \\ 32 & 75 \\ 4.6 \cdot 10^{-2} & 4.6 \cdot 10^{-2} \\ 4.6 \cdot 10^{-2} & 4.6 \cdot 10^{-2} \\ 10 & 20 \\ 10 & 22 \\ 1.3 \cdot 10^{-2} & 1.3 \cdot 10^{-2} \end{pmatrix} \cdot \frac{mm}{yr} \quad S_e := \begin{pmatrix} 0.13 & 0.13 \\ 0.13 & 0.13 \\ 0.13 & 0.13 \\ 0.13 & 0.13 \\ 0.12 & 0.12 \\ 0.12 & 0.12 \\ 0.13 & 0.13 \\ 0.13 & 0.13 \\ 0.13 & 0.13 \end{pmatrix}$$

Calculate the volumetric moisture content for each case ((Fang 1991, p. 251)):

$\Theta := \phi \cdot S_e$

$$\Theta = \begin{pmatrix} 0.07085 & 0.07085 \\ 0.07085 & 0.07085 \\ 0.07085 & 0.07085 \\ 0.07085 & 0.07085 \\ 0.0654 & 0.0654 \\ 0.0654 & 0.0654 \\ 0.07085 & 0.07085 \\ 0.07085 & 0.07085 \\ 0.07085 & 0.07085 \end{pmatrix}$$

Use index calculations to calculate the diffusion coefficient from Equations (3),(5),(6) and (12).

$i := 0..8$

$j := 0..1$

$$De_{i,j} := \frac{(\Theta_{i,j})^3}{\phi^{0.7}} \cdot Dwl + \lambda \cdot V_{i,j}$$

$$D_{i,j} := \frac{De_{i,j}}{\Theta_{i,j}}$$

$$Dwl = 0.0722654 \frac{m^2}{yr}$$

$$\begin{pmatrix} 1 \\ 2 \\ 3 \\ 4 \\ 9 \\ 10 \\ 11 \\ 12 \\ 13 \end{pmatrix} De = \begin{pmatrix} 3.139 \times 10^{-3} & 7.439 \times 10^{-3} \\ 3.339 \times 10^{-3} & 7.739 \times 10^{-3} \\ 3.339 \times 10^{-3} & 7.739 \times 10^{-3} \\ 3.239 \times 10^{-3} & 7.539 \times 10^{-3} \\ 3.552 \times 10^{-5} & 3.552 \times 10^{-5} \\ 3.552 \times 10^{-5} & 3.552 \times 10^{-5} \\ 1.039 \times 10^{-3} & 2.039 \times 10^{-3} \\ 1.039 \times 10^{-3} & 2.239 \times 10^{-3} \\ 4.061 \times 10^{-5} & 4.061 \times 10^{-5} \end{pmatrix} \frac{m^2}{yr} \quad D = \begin{pmatrix} 0.044 & 0.105 \\ 0.047 & 0.109 \\ 0.047 & 0.109 \\ 0.046 & 0.106 \\ 5.431 \times 10^{-4} & 5.431 \times 10^{-4} \\ 5.431 \times 10^{-4} & 5.431 \times 10^{-4} \\ 0.015 & 0.029 \\ 0.015 & 0.032 \\ 5.731 \times 10^{-4} & 5.731 \times 10^{-4} \end{pmatrix} \frac{m^2}{yr}$$

Plot the results. Define a log function for purposes of plotting results. The log function is used to define fewer points for the breakthrough curve over time. It defines the range of validity. The range selected below is chosen to define the breakthrough curve. The range statement (MathSoft, 1998, page 135) is used throughout the calculation. The function statement is used to plot each curve throughout the calculation.

$$logt := -9, -8.9 .. 7$$

$$t(logt) := 10^{logt} \cdot yr$$

The porewater velocity is set to V m/sec. and the diffusion coefficient equals the diffusion coefficient presented above. Compare the base case at the center of the model to the adjacent column. Plot the base case analysis in Figure IV-2.

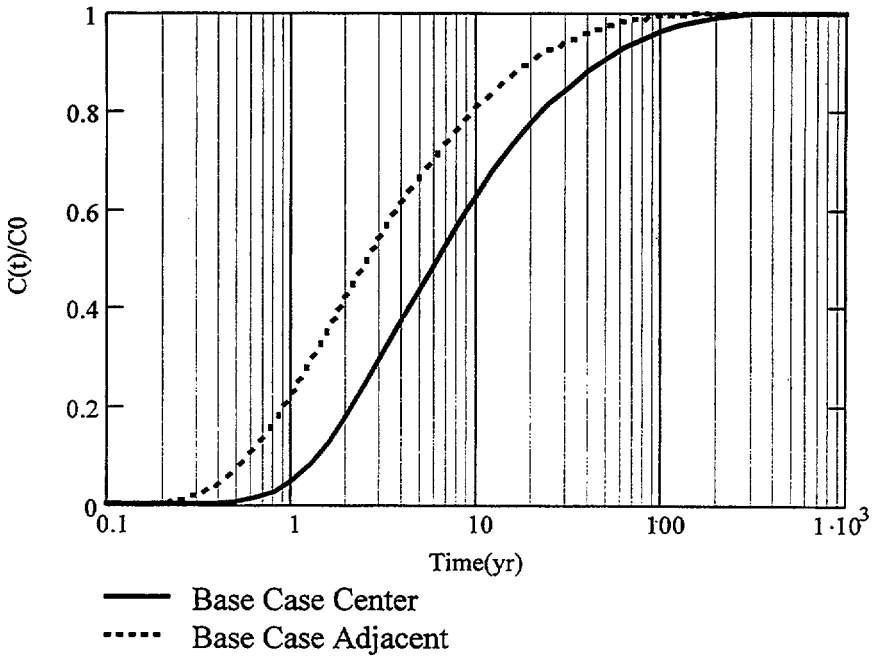

Figure IV-2 Breakthrough for One Dimensional Advection/Dispersion/Diffusion for the Base Case (Case 1)

Plot the effects of sand drains on the cases for the base case and fracture plugging in Figure IV-3.

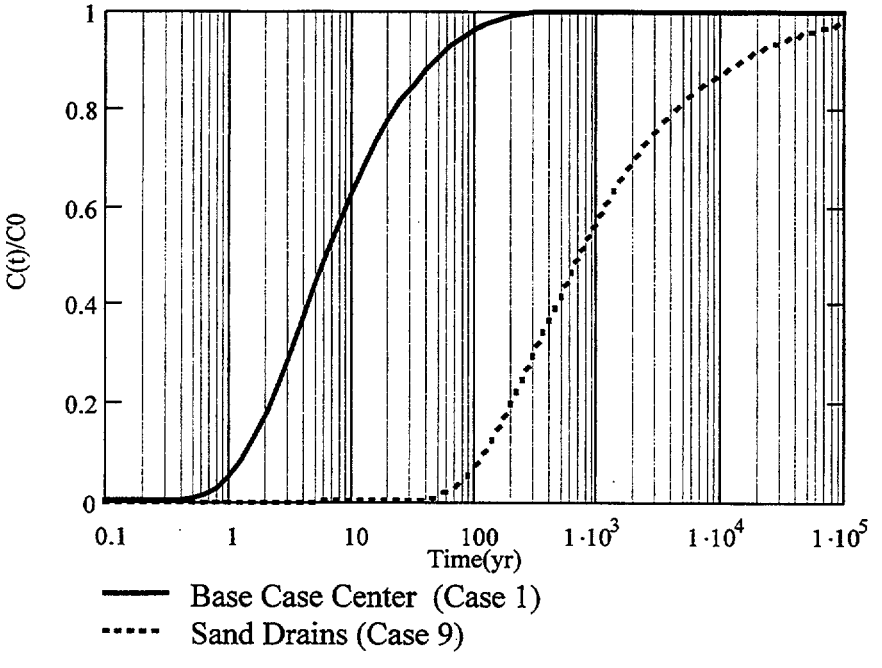

Figure IV-3 Effect of Sand Drains on Breakthrough

Compare the breakthrough time for the glacial climate to the present day climate in Figure IV-4.

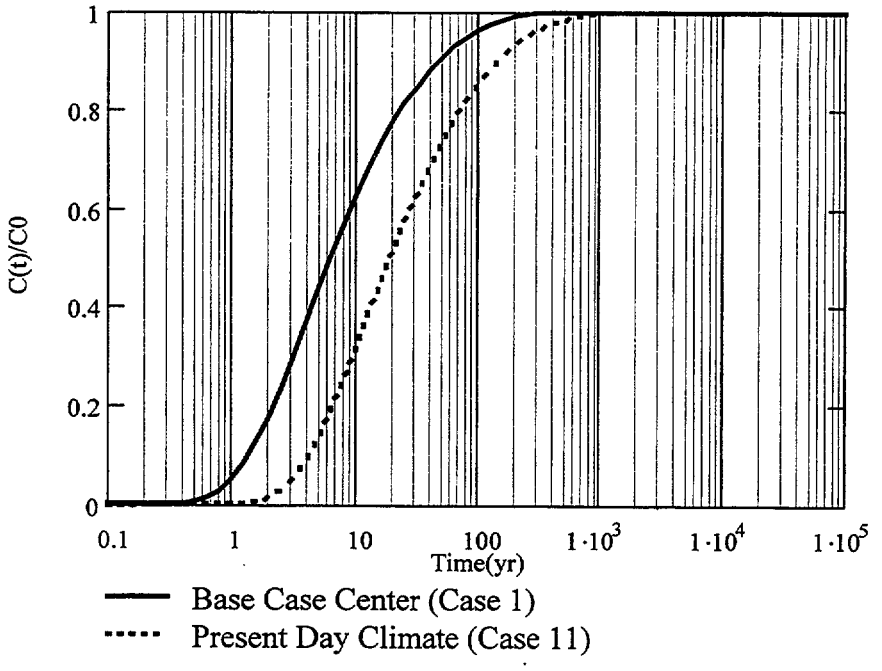

Figure IV-4 Effect of Climate on Breakthrough

Compare the case of sand drains for the present day climate to the case without sand drains for the present day climate in Figure IV-5.

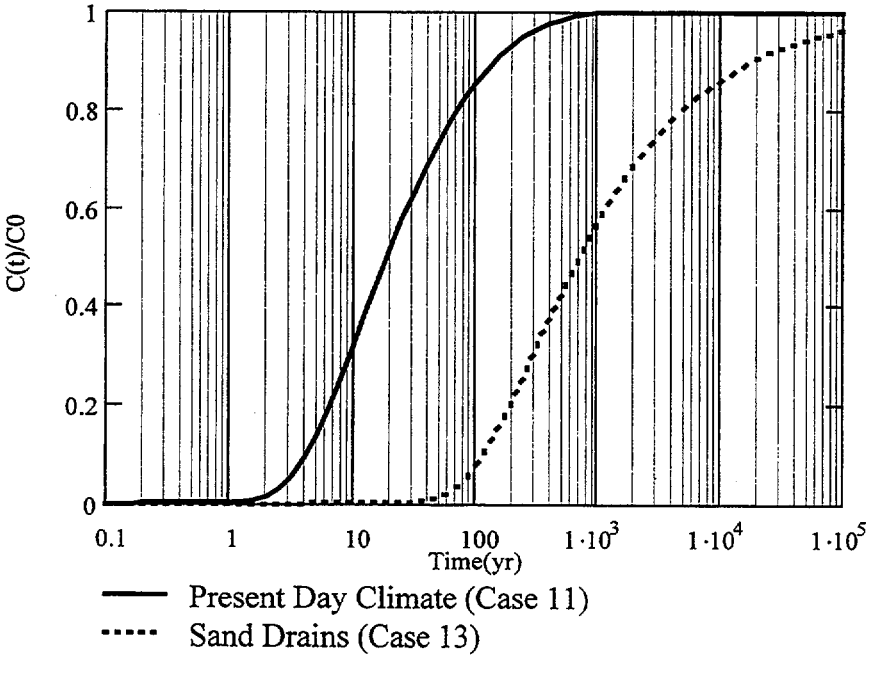

Figure IV-5 Effect of Sand Drains for the Present Day Climate

ATTACHMENT V

VALIDATION OF CRYSTAL BALL ROUTINES USED IN THE EXCEL SPREADSHEET CALLED ONE-DIMENSIONAL-FLOW_V.1.XLS

V.1 VALIDATION OF CRYSTAL BALL CALCULATIONS

The reports generated by the Crystal Ball routine, are contained on floppy (See Attachment III for list of computer files). The Excel spreadsheet, containing the Crystal Ball routine, entitled *One-dimensional-flow_V.1.xls* is contained on a floppy. The distribution of partition coefficients was modified each time to generate the Crystal Ball Reports. A sample problem testing Crystal Ball's proper multiplication and division of two uniformly distributed variables is contained on a floppy with filename titled *Verification of Crystal Ball.xls.* The results of this test are presented in Table V-1, and are compared to the analytical solution described in V.2.

Table V-1. Crystal Ball Test Results

Forecast: Distribution 1x2 **Cell: F8**

Summary:
Display Range is from 75.00 to 375.00
Entire Range is from 77.84 to 366.83
After 1,000 Trials, the Std. Error of the Mean is 2.10

Statistics:	Value
Trials	1000
Mean	200.33
Median	195.17
Mode	---
Standard Deviation	66.41
Variance	4,410.81
Skewness	0.34
Kurtosis	2.29
Coeff. of Variability	0.33
Range Minimum	77.84
Range Maximum	366.83
Range Width	288.99
Mean Std. Error	2.10

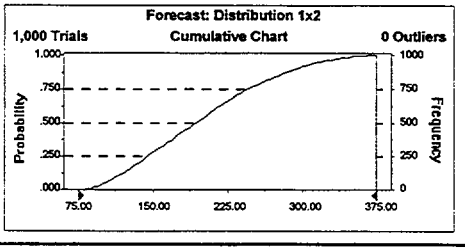

Table V-1. Crystal Ball Test Results (continued)

Forecast: Distribution 1/2 **Cell: H8**

Summary:

Display Range is from 0.20 to 1.00
Entire Range is from 0.20 to 0.97
After 1,000 Trials, the Std. Error of the Mean is 0.01

Statistics:	Value
Trials	1000
Mean	0.51
Median	0.49
Mode	---
Standard Deviation	0.16
Variance	0.03
Skewness	0.35
Kurtosis	2.40
Coeff. of Variability	0.32
Range Minimum	0.20
Range Maximum	0.97
Range Width	0.77
Mean Std. Error	0.01

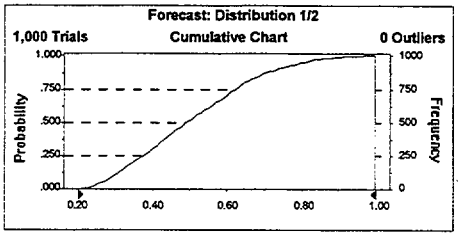

Table V-1. Crystal Ball Test Results (continued)

Forecast: Distribution 1 **Cell: B8**

Summary:

Display Range is from 5.00 to 15.00
Entire Range is from 5.01 to 14.99
After 1,000 Trials, the Std. Error of the Mean is 0.09

Statistics:	Value
Trials	1000
Mean	10.00
Median	10.00
Mode	---
Standard Deviation	2.89
Variance	8.34
Skewness	0.00
Kurtosis	1.80
Coeff. of Variability	0.29
Range Minimum	5.01
Range Maximum	14.99
Range Width	9.99
Mean Std. Error	0.09

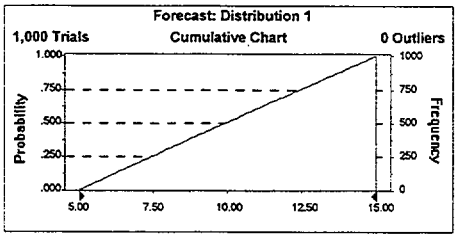

Table V-1. Crystal Ball Test Results (continued)

Forecast: Distribution 2 **Cell: D8**

Summary:
Display Range is from 15.00 to 25.00
Entire Range is from 15.01 to 25.00
After 1,000 Trials, the Std. Error of the Mean is 0.09

Statistics:	Value
Trials	1000
Mean	20.00
Median	19.99
Mode	---
Standard Deviation	2.89
Variance	8.34
Skewness	0.00
Kurtosis	1.80
Coeff. of Variability	0.14
Range Minimum	15.01
Range Maximum	25.00
Range Width	9.99
Mean Std. Error	0.09

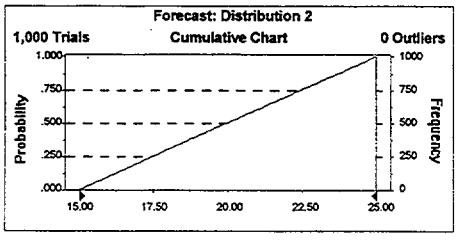

Table V-1. Crystal Ball Test Results (continued)

Assumptions

Assumption: Distribution 1 **Cell: B8**

Uniform distribution with parameters:

Minimum	5.00
Maximum	15.00

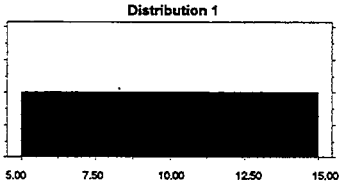

Mean value in simulation was 10.00

Assumption: Distribution 2 **Cell: D8**

Uniform distribution with parameters:

Minimum	15.00
Maximum	25.00

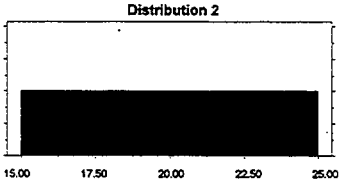

Mean value in simulation was 20.00

End of Assumptions

V.2 COMPARISON OF CRYSTAL BALL TEST RESULTS WITH ANALYTICAL SOLUTIONS

The following paragraphs provide a verification of the Crystal Ball routine. The verification problems consist of (1) generating a random variate x_1 according to a uniform distribution over the range from 5 to 15; (See Section V.1 for Distribution 1) (2) generating a second random variate x_2 over the range from 15 to 25 (See Sections V.1 for Distribution 2); (3) generating through Monte Carlo simulation and Latin Hypercube sampling a variate equal to the product of x_1 and x_2 ; and (4) generating through Monte Carlo simulation and Latin Hypercube sampling a variate equal to the division of x_1 by x_2 (See Sections V.1 for Distribution 1x2, and Distribution 1/2 respectively).

For Cases (1) and (2) presented above, theoretical values can be used for comparison of the statistics for expectation, variance, skewness, and kurtosis (Hahn and Shapiro 1968 pp. 126 - 128). For Cases (3) and (4), a closed form solution can be derived for the expected value and variance by generating system moments for the component variables x_1 and x_2 that are

uncorrelated (Hahn and Shapiro 1968, pp. 231). Assign the range for the uniform distribution of variable x_1

$\mu x1_0 := 5$

$\mu x1_1 := 15$

The expected value Ex1 and variance Varx1 for x_1 are given by the formula (Hahn and Shapiro 1968 p. 128):

$$Ex1 := \frac{\mu x1_0 + \mu x1_1}{2}$$

$$Varx1 := \frac{(\mu x1_0 - \mu x1_1)^2}{12}$$

$Ex1 = 10$

$Varx1 = 8.333$

$\sqrt{Varx1} = 2.887$

Assign the range for the uniform distribution x_2

$\mu x2_0 := 15$

$\mu x2_1 := 25$

The expected value Ex2 and variance Varx2 for x_2 are given by the formula (Hahn and Shapiro 1968 p. 128):

$$Ex2 := \frac{\mu x2_0 + \mu x2_1}{2}$$

$$Varx2 := \frac{(\mu x2_0 - \mu x2_1)^2}{12}$$

$Ex2 = 20$

$Varx2 = 8.333$

$\sqrt{Varx2} = 2.887$

The skewness equals the square root of the parameter β_1 equals zero in both cases since the distributions are symmetrical distributions about the expected values. Further, the theoretical value for the kurtosis β_2 equals 1.8. The values as generated from 1000 trials in Crystal Ball are presented in Table V-2.

Table V-2 Comparison of Results for Variables X_1 and X_2

Statistic	Theoretical x_1	Crystal Ball x_1	Theoretical x_2	Crystal Ball x_2
Trials	NA	1000	NA	1000
Mean	10	10	20	20
Standard Deviation	2.89	2.89	2.89	2.89
Variance	8.33	8.34	8.33	8.34
Skewness	0	0	0	0
Kurtosis	1.8	1.8	1.8	1.8
Range Minimum	5	5.01	15	15.01
Range Maximum	15	14.99	25	25

Note that the values presented above are in general agreement with minor differences attributable to sampling errors for one thousand realizations.

Consider the third case which corresponds to the product of x_1 and x_2. The mean system performance which in this case is $x_1 * x_2$ is developed from the analytical solution expressed by Hahn and Shapiro (1968, p. 229):

$$z = h(x_1, x_2)$$

$$h(x_1, x_2) = x_1 \cdot x_2$$

$$E(z) = h(E(x_1), E(x_2)) + \frac{1}{2} \cdot \sum_{i=1}^{2} \left(\frac{d^2}{dx_i^2} h \right) \cdot Var(x_i)$$

The analytical solution for the variance for the third case is developed from the analytical solution expressed by Hahn and Shapiro (1968, p. 231):

$$Var(z) = \sum_{i=1}^{2} \left(\frac{d}{dx_i} h \right)^2 \cdot Var(x_i) + \sum_{i=1}^{2} \left(\frac{d}{dx_i} h \right) \cdot \left(\frac{d^2}{dx_i^2} h \right) \cdot \mu_3(x_i)$$

In the analytical solutions presented above for the third case, it is noted that the second order derivatives are zero, and since the skewness is zero for the symmetrical uniform distribution, the third moment must be zero as given by the definition of skewness (Hahn and Shapiro 1968, p. 45). Therefore the analytical solutions for the third case simplify to:

$$E(z) = E(x_1) \cdot E(x_2)$$

$Ez := Ex1 \cdot Ex$

$Ez = 200$

$$Var(z) = \sum_{i=1}^{2} \left(\frac{d}{dx_i} h \right)^2 \cdot Var(x_i)$$

$$Var(z) = E(x_2)^2 \cdot Var(x_1) + E(x_1)^2 \cdot Var(x_2)$$

$Varz := Ex2^2 \cdot Varx1 + Ex1^2 \cdot Varx$

$Varz = 4.167 \times 10^3$

$\sqrt{Varz} = 64.55$

Consider the fourth case which corresponds to the division of x_1 by x_2. The mean system performance which in this case is x_1/x_2 is developed from the analytical solution expressed by Hahn and Shapiro (1968, p. 229):

$$z = h(x_1, x_2)$$

$$h(x_1, x_2) = \frac{x_1}{x_2}$$

$$E(z) = h(E(x_1), E(x_2)) + \frac{1}{2} \cdot \sum_{i=1}^{2} \left(\frac{d^2}{dx_i^2} h \right) \cdot Var(x_i)$$

In this case the second order derivative for the divisor is not zero, and the analytical solution for the expected value becomes

$$E(z) = \frac{E(x_1)}{E(x_2)} + \frac{1}{2} \cdot \left(2 \cdot \frac{E(x_1)}{E(x_2)^3} \right) \cdot Var(x_2)$$

$$Ez := \frac{Ex1}{Ex2} + \frac{Ex1}{Ex2^3} \cdot Varx$$

$$Ez = 0.51$$

The analytical solution for the variance for the fourth case is again developed from the analytical solution expressed by Hahn and Shapiro (1968, p. 231):

$$Var(z) = \sum_{i=1}^{2} \left(\frac{d}{dx_i} h \right)^2 \cdot Var(x_i) + \sum_{i=1}^{2} \left(\frac{d}{dx_i} h \right) \cdot \left(\frac{d^2}{dx_i^2} h \right) \cdot \mu_3(x_i)$$

In the analytical solutions presented above for the third case, it is noted that the skewness is zero for the symmetrical uniform distribution, the third moment must be zero as given by the definition of skewness (Hahn and Shapiro 1968, p. 45). Therefore the analytical solutions for the fourth case simplify to

$$Var(z) = \sum_{i=1}^{2} \left(\frac{d}{dx_i} h \right)^2 \cdot Var(x_i)$$

$$Var(z) = \left(\frac{1}{E(x_2)} \right)^2 \cdot Var(x_1) + \left(\frac{-E(x_1)}{E(x_2)^2} \right)^2 \cdot Var(x_2)$$

Substituting the values calculated above

$$Varz := \left(\frac{1}{Ex2} \right)^2 \cdot Varx1 + \left(\frac{Ex1}{Ex2^2} \right)^2 \cdot Varx$$

$$Varz = 0.026$$

$$\sqrt{Varz} = 0.161$$

Table V-3 Comparison of Results for Product and Division Functions

Statistic	Theoretical $x_1 \cdot x_2$	Crystal Ball $x_1 \cdot x_2$	Theoretical x_1/x_2	Crystal Ball x_1/x_2
Trials	NA	1000	NA	1000
Mean	200	200.33	0.51	0.51
Standard Deviation	64.55	66.41	0.16	0.16
Variance	4.17E+03	4.41E+03	0.026	0.03

The results of the analysis from Crystal Ball for 1,000 realizations for the third and fourth cases are in general agreement with the results from closed form analytical solutions. The differences in values as presented in Table V-3 are due to sampling errors that occur with any synthetic sampling.